Carbon Nanodots for Cell Imaging

Xiaodong Zhang, Xiaokai Chen, and Fu-Gen Wu

1 Introduction

Carbon nanodots (CNDs), also known as carbon dots (CDs), graphene quantum dots (GQDs), carbon quantum dots (CQDs), carbonized polymer dots, or C-dots, are zero-dimensional fluorescent carbonaceous nanomaterials with a typical size of <10 nm [1–3]. CNDs were first discovered from the purification of single-walled carbon nanotube fragments in 2004 [4], and they have been widely investigated since pure CNDs with multicolor emission were prepared by Sun et al. [5].

Generally, CNDs have an internal core composed of sp^2-hybridized carbon atoms, and an external surface with various functional groups such as amino, carboxyl, hydroxyl, epoxy, ether, and carbonyl groups [6–8]. Both the conjugated carbon core and surface defects can affect the optical properties, conductivity, and catalytic activity of the CNDs [9]. Many CNDs possess interesting excitation-dependent emission properties [10–13], which means that the emission wavelengths have redshifts with the increasing excitation wavelengths. It is believed that the distinct optical properties of CNDs are highly related to their carbon core and surface defects [9].

Compared to other fluorescent materials, CNDs have several advantages that are beneficial for biomedical applications. First, most CNDs have good water-dispersity due to the abundant hydrophilic groups on their surfaces, which makes further hydrophilic modification unnecessary [14–16]. Second, their surface groups such as amino and carboxyl groups endow CNDs with the convenience of conjugating with functional molecules such as targeting ligands and drugs [17–19]. Third, CNDs have a strong anti-photobleaching property [20–22]. For example, it was reported that the fluorescence intensity of CNDs prepared by glycerol and (3-aminopropyl) triethoxysilane (APTES) only decreased to ~60% after 200 min ultraviolet (UV) light irradiation [23]. In contrast, other fluorescent probes including CdTe quantum dots, gold nanoclusters (Au NCs), and fluorescein isothiocyanate (FITC) were almost completely quenched under the same condition. Fourth, CNDs can be facilely prepared at a low cost. They have been synthesized from various precursors such as small organic molecules [24, 25], polymers [26, 27], bulk carbon [28], cells [29, 30], and biomass resources [3] through different approaches. Acidic oxidation, hydrothermal/solvothermal route, microwave-assisted synthesis, and electrochemical preparation are the commonly used inexpensive approaches for the preparation of CNDs [9, 31]. Fifth, the optical properties of CNDs can be tuned through changing the precursors and reaction conditions such as temperature and time

X. Zhang · X. Chen · F.-G. Wu (✉)
State Key Laboratory of Bioelectronics, School of Biological Science and Medical Engineering, Southeast University, Nanjing, Jiangsu, China
e-mail: wufg@seu.edu.cn

F.-G. Wu (ed.), *Fluorescent Materials for Cell Imaging*, https://doi.org/10.1007/978-981-15-5062-1_3

[32]. For example, Jiang et al. used three isomers of phenylenediamines (including *m*-phenylenediamine, *o*-phenylenediamine, and *p*-phenylenediamine) as the carbon sources to obtain blue-, green-, and red-emitting CNDs, respectively [33]. Zhang et al. reported that the fluorescence color of the CNDs prepared by *L*-valine (as the carbon sources) and H_3PO_4 (as the oxidant) could be changed from green to yellow through prolonging the reaction time [34].

Owing to their superior properties, CNDs have broad applications in catalysis [35], electronics [36], sensing [37], drug delivery [38], and bioimaging [39, 40]. In this chapter, we will summarize the use of CNDs in imaging a variety of cells, including mammalian cells, microbial cells, and plant cells.

2 Preparation of CNDs

"Bottom-up" and "top-down" approaches are the two commonly used methods to prepare nanoparticles. CNDs as fluorescent nanomaterials can also be synthesized via the two strategies. The "bottom-up" approach to synthesize CNDs is realized through the carbonization of small organic molecules or the stepwise chemical fusion of small aromatic molecules, while the "top-down" approach is achieved by breaking down carbonaceous materials. To realize the "bottom-up" or "top-down" synthesis of CNDs, hydrothermal/solvothermal, microwave-assisted, electrochemical, and acidic oxidation methods have been proposed.

2.1 Hydrothermal/Solvothermal Method

Hydrothermal/solvothermal method, as the most popular "bottom-up" approach for synthesizing CNDs, only requires an inexpensive heating system and a hydrothermal reactor, and can realize the high-quality synthesis of CNDs with simple procedures [41–43]. The hydrothermal/solvothermal temperature used for the preparation of CNDs is usually in the range of 120–300 °C [9], and the reaction temperature and reaction time can largely affect the size and optical properties of the as-prepared CNDs [44, 45].

Zhang et al. prepared nitrogen-doped and fluorescence-tunable CNDs by a one-pot solvothermal reaction using CCl_4 and $NaNH_2$ [44]. They found that the size of the CNDs increased with increasing reaction time, and their excitation and emission wavelengths had a redshift when the reaction duration prolonged from 1 to 8 h. Li et al. demonstrated that the CNDs with different surface densities of amino groups and the excitation-dependent/excitation-independent fluorescence property could be prepared through controlling hydrothermal reaction temperature [45]. They found that the CNDs prepared at lower temperatures (e.g., 160 °C) had a higher surface density of amino groups with the excitation-independent fluorescence property. By comparison, the CNDs synthesized at higher temperatures (e.g., 240 °C) had a lower surface density of amino groups with the excitation-dependent fluorescence property.

Besides, the reaction solvent also plays an important role in the preparation of CNDs. For example, the CNDs obtained from *o*-phenylenediamine using the hydrothermal method had the maximum emission wavelength located at 567 nm under 420 nm excitation with a low photoluminescence quantum yield (PLQY) of 2% [46]. In contrast, the *o*-phenylenediamine-derived CNDs using ethanol as the reaction solvent had a much higher PLQY of 17.6% under 420 nm excitation [33].

2.2 Microwave-Assisted Method

Compared with the hydrothermal/solvothermal method, the microwave-assisted method is a much faster approach for the synthesis of nanomaterials with a reaction duration from minutes to tens of minutes [47–50]. The CNDs prepared via the microwave-assisted method usually have a narrow size distribution, which is mainly because microwave has a deep penetration depth and uniform heating performance. If the raw materials can form CNDs under

hydrothermal/solvothermal conditions, they may also be used to synthesize CNDs through the microwave-assisted method. However, the CNDs prepared by the two different approaches may have some differences.

Huang et al. prepared the CNDs using the mixture containing glycerol and (3-aminopropyl)triethoxysilane (APTES) under microwave irradiation within a short reaction period of 30 min [23]. After the incubation of these CNDs with HeLa cells, some dot-like fluorescence signals were observed in the cytoplasms. By contrast, the CNDs prepared using similar raw materials by the solvothermal method targeted the mitochondria after incubation with the HeLa cells, as demonstrated by our group [51].

2.3 Electrochemical Method

Compared with the above-mentioned "bottom-up" methods, the electrochemical method for the preparation of CNDs has some distinct advantages, such as low cost, low energy consumption, the capability of real-time monitoring of the CND formation, and large-scale production [52, 53]. Moreover, both thermally stable and unstable raw materials can be used to synthesize CNDs using the electrochemical method. Besides, the size and properties of the as-prepared CNDs can be tuned through changing the reaction conditions, such as electrode potential, electrolyte type, electrolyte concentration, and reaction time. For example, Deng et al. developed a simple method to prepare CNDs through the electrochemical carbonization of low-molecular-weight alcohols [54]. The size of the CNDs could be tuned by changing the electrode potential, and the fluorescence emission of the resultant CNDs was excitation- and size-dependent.

Besides its use for the "bottom-up" synthesis of CNDs, the electrochemical method can also serve as a "top-down" way to produce CNDs [55, 56]. It is proposed that OH• and O• radicals formed from the anodic oxidation of water can oxidize bulk carbon sources, leading to the formation of small hydroxylated carbon particles [57]. To introduce functional groups or heteroatoms into the CNDs, choosing different electrolyte solutions is considered as an available way [58, 59]. For instance, to prepare nitrogen (N)-doped CNDs, Li et al. used N-containing tetrabutylammonium perchlorate in acetonitrile as the electrolyte to introduce N atoms into the resultant CNDs [58].

2.4 Acidic Oxidation Method

Besides the electrochemical exfoliation, the acidic oxidation method is also a common "top-down" way to produce CNDs. The acidic oxidation method has been successfully used to exfoliate CNDs from various carbon sources, such as carbon fibers [60], carbon nanotubes [61], nanodiamonds [62], graphite oxide [63], plant soot [64], coal [65], carbon black [66], and activated carbon [67]. Large-quantity synthesis of CNDs from bulk carbon sources can be realized by this method. Furthermore, acidic treatment usually endows CNDs with negatively charged groups on their surfaces, making them hydrophilic and easy to be further modified. For example, Zhang et al. synthesized water-dispersible CNDs with tunable photoluminescence via the one-pot acidic oxidation of nanodiamonds using H_2SO_4, HNO_3, and $KMnO_4$ [62]. During the oxidation process, many functional groups such as carboxyl and hydroxyl groups were introduced on the surface of the CNDs. In addition, the CNDs were successfully used in cytoplasm imaging due to its excellent water dispersibility and biocompatibility.

3 CNDs for Mammalian Cell Imaging

Owing to their superior fluorescence properties and excellent biocompatibility, CNDs show great potential in biomedical applications. Imaging cells especially mammalian cells using CNDs is a hot research topic [68–70]. CNDs have been used to light up the whole cells or some parts of

the cells, and monitor the locations and concentrations of the molecules/ions in the cells. Besides, thanks to the presence of many reactive groups on their surfaces, CNDs can be modified with targeting moieties and realize selective imaging of the cells especially the cancer cells.

3.1 CNDs for Subcellular Imaging

In mammalian cells, various subcellular structures such as the nucleus, mitochondrion, lysosome, Golgi apparatus, endoplasmic reticulum, ribosome, and plasma membrane are essential components of the cells. Each subcellular structure performs its specialized role to support the fundamental cellular functions. Thus, visualization and monitoring of subcellular components are of great importance. Compared with other fluorescent probes, CNDs have many functional groups on their surfaces, enabling subcellular structure-targeting moieties to be easily conjugated with the CNDs. On the other hand, because a variety of carbon sources can be used for the preparation of CNDs, the as-prepared CNDs have different surface properties, and even have intrinsic subcellular structure-targeting ability without further modifications. Besides, CNDs have excellent photostability, making them suitable for the long-term monitoring of subcellular components. Additionally, CNDs can be facilely prepared with low cost, making them much cheaper than the commercial subcellular imaging probes.

3.1.1 CNDs for Nucleus/Nucleolus Imaging

Cell nucleus which contains the majority of cellular genetic materials acts as the brain of the cell. Thus, many efforts have been devoted to visualizing cell nuclei [71, 72]. However, the probes with large sizes are hard to enter the nuclei because of the presence of the small nuclear pores [73]. Thanks to their ultrasmall size and excellent fluorescence properties, CNDs show great potential in imaging cell nuclei.

As shown in Fig. 1, Yang et al. synthesized the amine group-containing CNDs, and functionalized the CNDs with nuclear localization signal (NLS) peptide through carboxyl–amine reaction for realizing cell nucleus imaging [74]. Besides, it has been reported that zwitterionic CNDs may have the intrinsic nucleus-targeting ability [75, 76]. For example, Jung et al. prepared zwitterionic CNDs using citric acid and β-alanine as raw materials [75]. The CNDs had excitation-dependent photoluminescence, which could monitor the cell nuclei in blue, green, and red fluorescence channels. Similarly, ascorbic acid and polyethyleneimine were used as raw materials to fabricate nitrogen-doped zwitterionic CNDs [76]. The as-prepared CNDs could also enter the cell nucleus without further modification.

As the largest structure in a nucleus, the nucleolus is the site of ribosome biogenesis, and plays an important role in the formation of signal recognition particles and the cellular response to stress [77, 78]. Several studies have reported that CNDs can enter the cell nuclei and even target the nucleoli [79–82].

Barbosa et al. found that the surface modification of the CNDs with ethylenediamine could endow the CNDs with the nucleolus-targeting ability [79]. Besides, CNDs with intrinsic nucleolus-imaging ability were also reported. For example, Kong et al. synthesized highly bright fluorescent CNDs by refluxing polyethylene glycol in the presence of sodium hydroxide, which were used to selectively stain cell nucleoli [80]. The nucleolus-targeting ability of the CNDs may be attributed to the large number of oxygen-containing functional groups on their surfaces, which make the CNDs easy to interact with the weakly alkaline chromatin of the nuclei rather than other subcellular structures. Our group reported the one-pot hydrothermal synthesis of nucleolus-targeting CNDs using *m*-phenylenediamine and *L*-cysteine [81]. Different from the commercial nucleolus-imaging probe SYTO RNASelect which can only be used to stain the nucleoli of the fixed cells, the as-prepared CNDs could realize nucleolus imaging in both fixed and living cells (Fig. 2), making it possible for the in situ monitoring of nucleolus-related biological behaviors. For the nucleolus-targeting mechanism of the CNDs, we found

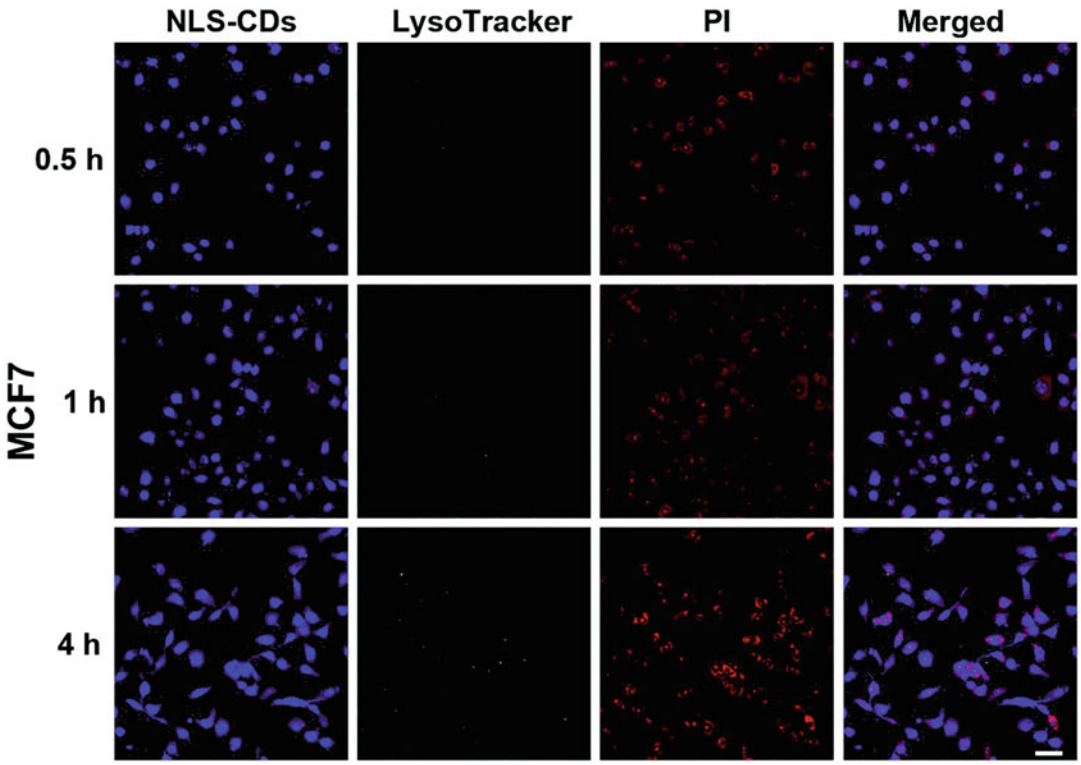

Fig. 1 Confocal microscopic images showing the nuclear imaging performance of NLS-conjugated CDs (NLS-CDs). Reprinted with permission from Ref. [74]. Copyright © 2015 Royal Society of Chemistry

that the CNDs could selectively bind to RNA instead of DNA after entering the nucleus. Furthermore, the fluorescence intensity of the CNDs was markedly increased after interaction with RNA, which makes the RNA-bound CNDs much brighter than free CNDs. Recently, we also found that the mixture of metal ions and *p*-phenylenediamine could form red-emitting CNDs after hydrothermal treatment, and the as-prepared CNDs could be used for the real-time and high-resolution fluorescence imaging of the nucleoli of living cells [82].

3.1.2 CNDs for Mitochondrial Imaging

Besides the cell nucleus, the mitochondrion is also an important organelle for the cell, because it is the "powerhouse" of the cell and is related to various cellular functions such as energy conversion, storage of calcium ions, and regulation of cellular metabolism [83]. Owing to the large membrane potential gradient of the mitochondrion, mitochondrion-targeting probes are usually positively charged, which enable the interaction of these probes with mitochondria.

Triphenylphosphonium (TPP), a commonly used mitochondrion-targeting ligand, was successfully conjugated with the CNDs derived from citric acid and urea [84]. The TPP-functionalized CNDs were used for both one- and two-photon mitochondrial imaging in living cells. Our group synthesized fluorescent CNDs through the hydrothermal treatment of chitosan, ethylenediamine, and mercaptosuccinic acid [85]. The as-prepared CNDs were endocytosed by the cells through the caveolae-mediated pathway and then specifically targeted mitochondria without further modification. We presumed that the raw materials mercaptosuccinic acid and chitosan/ethylenediamine could form delocalization structures and positively charged surfaces, respectively, which endowed the CNDs with excellent mitochondrion-targeting

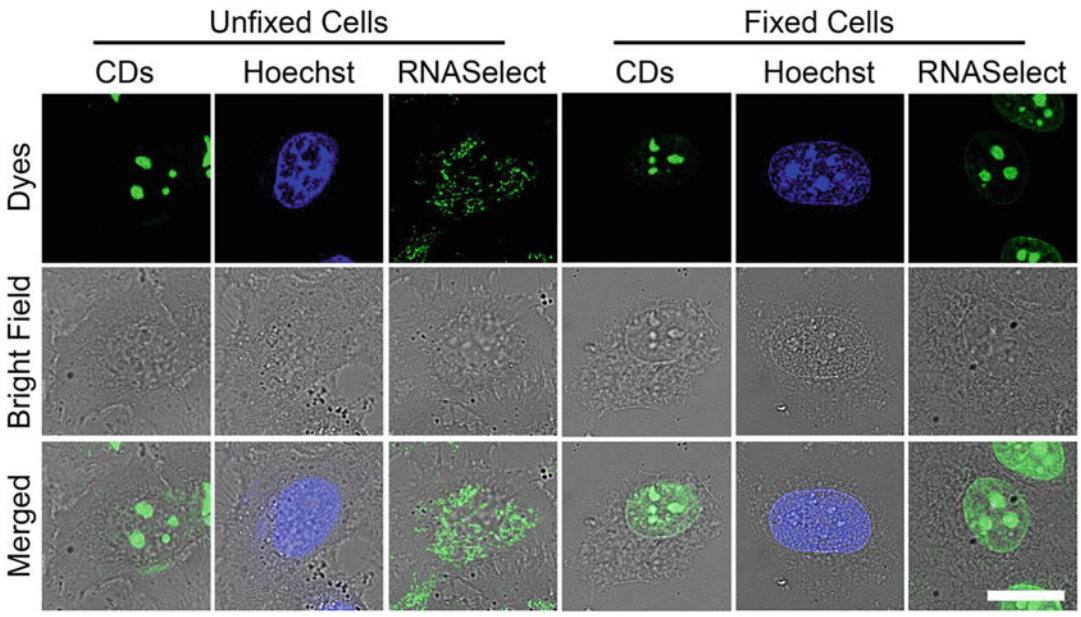

Fig. 2 Confocal microscopic images showing the nucleolus-imaging performance of CDs and SYTO RNASelect in unfixed and fixed cells. Reprinted with permission from Ref. [81]. Copyright © 2018 American Chemical Society

ability. Different from the commercial mitochondrial imaging dye Mito-Tracker which cannot be used to image mitochondria for a long time, the CNDs could firmly attach to mitochondria and realize long-term mitochondrial tracking for more than 24 h. Besides, our group prepared a series of CNDs with inherent mitochondrial targeting/imaging capability using the solvothermal treatment of glycerol and silane molecules (Fig. 3) [51]. The cationic (3-aminopropyl)trimethoxysilane (APTMS) CDs were easy to accumulate in mitochondria rather than in other organelles due to the large membrane potential of the mitochondria. Interestingly, the CNDs could effectively distinguish cancerous cells from normal ones due to the differences in the mitochondrial membrane potentials and uptake efficiencies of the two types of cells.

3.1.3 CNDs for Lysosomal Imaging

Lysosomes are the waste disposal system of cells and essential in various physiological processes (e.g., autophagy and protein degradation) [86–88]. Generally, acidotropic dyes and some large molecules are the two types of lysosome-targeting reagents. The former type usually includes weakly basic amines, such as morpholine and commercial lysosomal imaging agents Lyso-Tracker/Lyso-Sensor probes. They can target the lysosomes due to their acidic environment. The latter one (i.e., Alexa Fluor 594-conjugated dextran and BODIPY-conjugated bovine serum albumin) can be internalized by cells and enter the lysosomes through the endo-lysosomal pathway.

Taking advantage of the lysosome-targeting ability of morpholine derivatives, Wu et al. modified the CNDs (prepared by citric acid and polyethylenimine) with morpholine groups for long-term lysosomal imaging [89]. Similar to the morpholine derivatives, the ruthenium (II) complex (Ru1) is also a ligand that can target lysosomes. Based on this, Zhang et al. constructed the nanohybrids composed of CNDs and Ru1 for one- and two-photon imaging of lysosomes [90]. Besides, it was reported that some amine-containing CNDs have the intrinsic lysosome-targeting ability. For example, E et al. found that amine group-functionalized CNDs prepared from citric acid and urea could image the lysosomes [91]. Zhang et al. used *p*-benzoquinone and ethanediamine to prepare highly

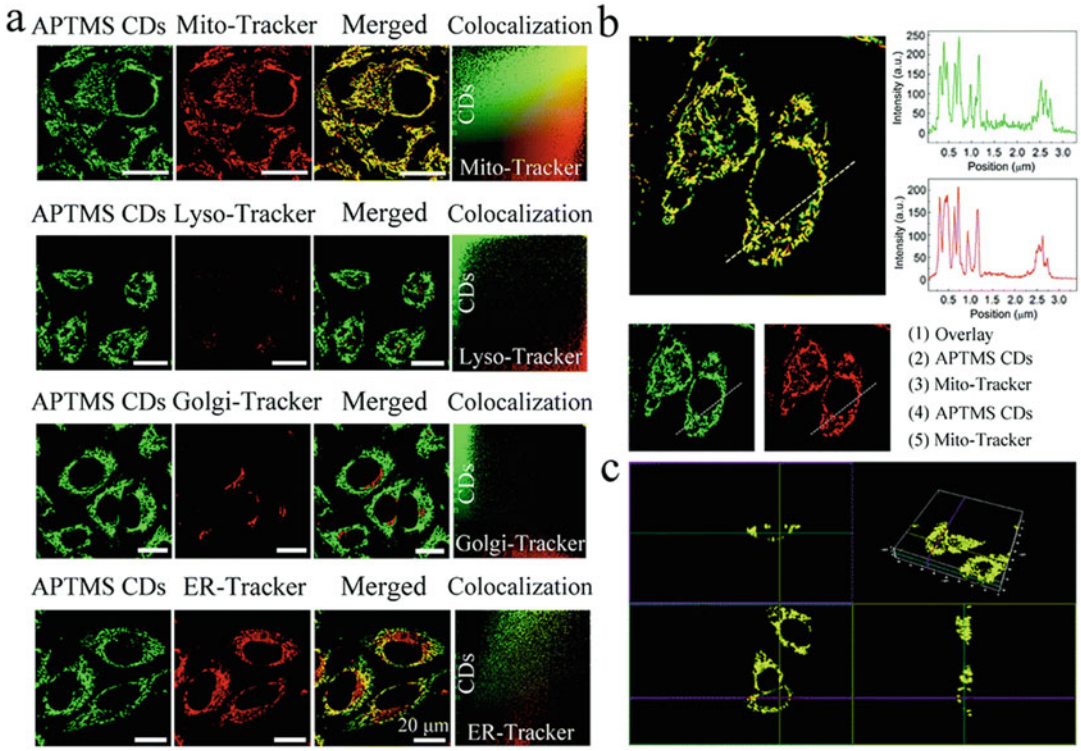

Fig. 3 (**a**) Confocal microscopic images showing the colocalization of APTMS CDs with Mito-Tracker, Lyso-Tracker, Golgi-Tracker, or ER-Tracker. (**b**) Fluorescence distribution of APTMS CDs and Mito-Tracker. (**c**) Three dimensional merged confocal microscopic images of Mito-Tracker- and APTMS CD-costained HeLa cells viewed via multiple cross sections. Reprinted with permission from Ref. [51]. Copyright © 2017 Royal Society of Chemistry

photoluminescent lysosome-targeting CNDs [92]. They believed that the lysosome-targeting ability of the CNDs was attributed to their abundant hydrophilic groups, especially the amine groups. Liu et al. reported the synthesis of lysosome-targeting CNDs using dexamethasone and 1,2,4,5-tetraaminobenzene as the raw materials [93]. The authors attributed the lysosomal targeting performance of the CNDs to the acidotropic effect of the amine groups on the surface of the CNDs. Chen et al. found that the surface amine groups could improve the lysosome-targeting specificity of the CNDs that were prepared from methionine and citric acid and further modified by a naphthalimide derivative [94]. Zhao et al. synthesized lysosome-targetable CNDs using 1,3,6-trinitropyrene and NaOH without further modification [95]. They also believed that the amine groups endowed the CNDs with lysosome-targeting ability. Recently, Qin et al. developed a novel fluorescent probe based on CNDs prepared from *N*-methyl-1,2-phenylenediamine hydrochloride [96]. The CNDs were non-fluorescent in water, but emitted strong yellow fluorescence in cells. Besides, the CNDs had good lysosome-targeting ability due to the presence of amine groups, making them suitable for fast imaging lysosomes without washing steps. Singh et al. reported a simple and facile hydrothermal method to synthesize the CNDs using neem root extracts as the raw materials [97]. The as-prepared CNDs with strong lysosomal specificity were suitable for structured illumination microscopy and two-photon microscopy (Fig. 4). The authors presumed that the presence of the ether, carboxyl, and amino groups on the surface of the CNDs might ensure the appropriate lipophilicity for lysosomal targeting. Similarly, Guo et al. used a facile microwave-assisted method to prepare green-emitting CNDs with

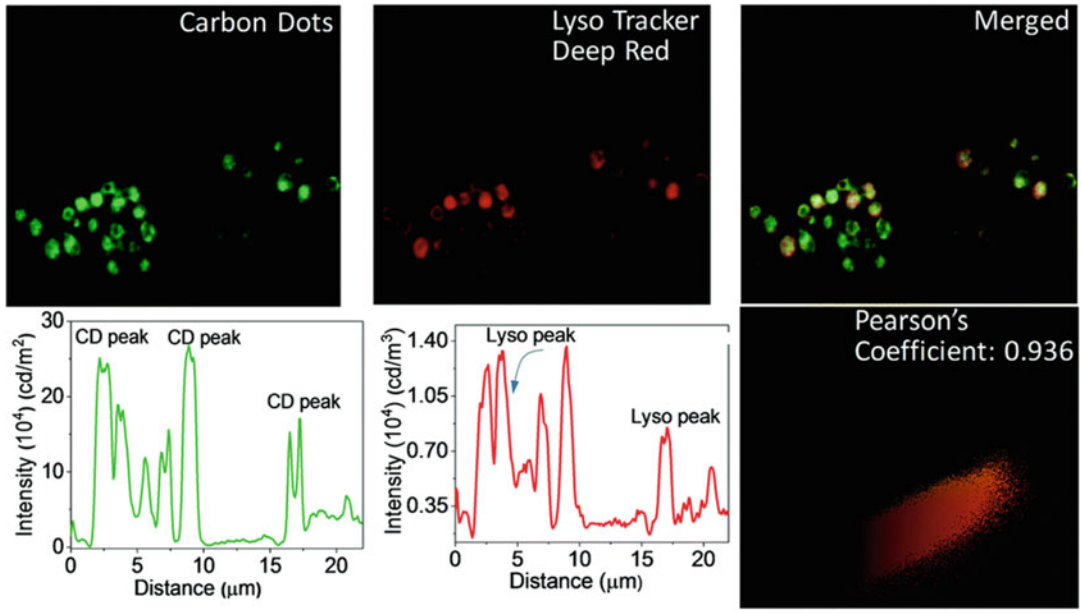

Fig. 4 Evaluation of the colocalization of the CNDs (carbon dots) with Lyso-Tracker Deep Red probes in RAW cells. Reprinted with permission from Ref. [97]. Copyright © 2019 Royal Society of Chemistry

intrinsic lysosome-targeting ability using citric acid and *N*,*N*-dimethylaniline as the raw materials [98]. The CNDs could specifically monitor the lysosomes in various cell lines for more than 48 h, and even stain the lysosomes in apoptotic cells and fixed cells.

3.1.4 CNDs for Golgi Apparatus Imaging

The Golgi apparatus is a crucial eukaryotic organelle for biogenesis, secretion, and intracellular distribution of a wide range of macromolecules [99]. The morphological change of the Golgi apparatus is related to external stimuli, which can thus effectively reflect the physiological state of cells. As a result, it is urgently needed to develop new fluorescent probes capable of real-time monitoring the morphology of the Golgi apparatus.

Li et al. developed a pyrolysis method to prepare chiral CNDs using citric acid and *L*-cysteine as the carbon sources [100]. The chiral CNDs (termed LC-CQDs) had a high PLQY of 68% and showed excellent photostability. Moreover, as shown in Fig. 5, long-time Golgi apparatus targeting and monitoring was realized using the CNDs. The authors believed that the Golgi apparatus-targeting ability of the CNDs was attributed to the presence of the cysteine residues on their surfaces. In another work, Wang et al. reported a simple molecular fusion route for industrial production of sulfonated CNDs from 1,3,6-trinitropyrene [101]. The 1,3,6-trinitropyrene molecules were completely converted into the CNDs without byproducts after a green sulfonation reaction at a low hydrothermal temperature of 130 °C. Then, the CNDs were used to target and visualize the Golgi apparatuses in living cells.

3.2 CNDs for Monitoring the pH and Ions/Molecules in the Cells

3.2.1 CNDs for Intracellular pH Sensing

Intracellular pH modulates the functions of many organelles and plays a pivotal role in biological systems, such as cell proliferation and apoptosis, ion transport, and muscle contraction [102]. As a result, it is essential to monitor the pH distribution and change in living cells. CNDs with good

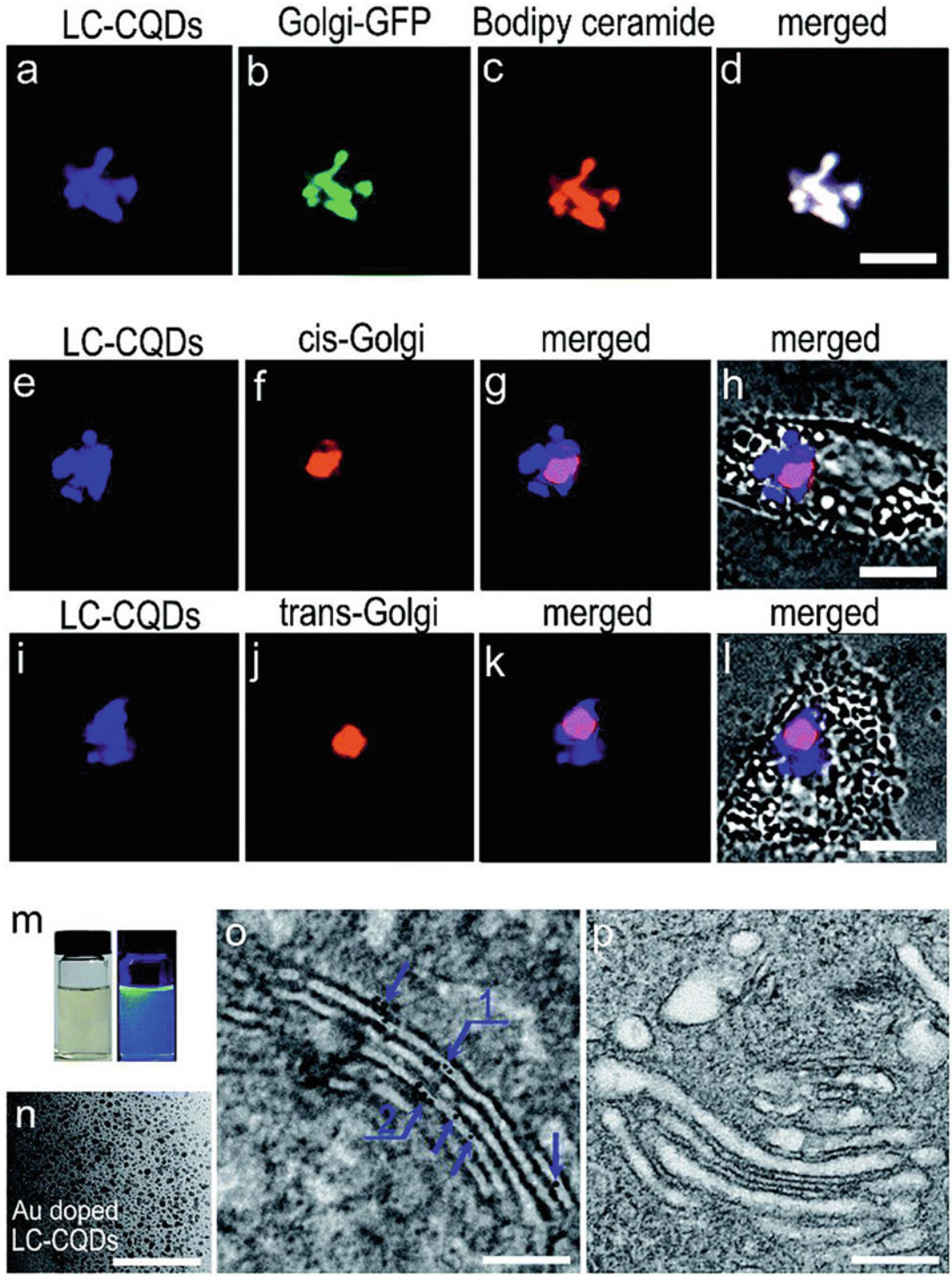

Fig. 5 Evaluation of the Golgi apparatus-targeting ability of the LC-CQDs. (**a**–**d**) Fluorescence images of the LC-CQDs (blue), Golgi-GFP (green, Golgi apparatus-specific green fluorescent protein), and Bodipy ceramide (red, a commercial dye for Golgi apparatus) in a HEp-2 cell. (**e**–**h**) Fluorescence images showing the colocalization of the LC-CQDs and the cis-Golgi. (**i**–**l**) Fluorescence images showing the colocalization of the LC-CQDs and the trans-Golgi. (**m**) Photographs of the Au-doped LC-CQDs under illumination by white light (left) and UV (365 nm) light (right). (**n**) TEM image of the Au-doped LC-CQDs. (**o**, **p**) TEM images of the Golgi apparatus of the cells incubated with (**o**) and without (**p**) Au-doped LC-CQDs. Reprinted with permission from Ref. [100]. Copyright © 2017 Royal Society of Chemistry

water-dispersity usually have numerous pH-sensitive groups such as amino groups and carboxyl groups on their surfaces, endowing the fluorescence of CNDs with pH responsiveness [10, 14, 92, 103–106].

Zhang et al. developed a simple method to prepare highly photoluminescent CNDs by mixing *p*-benzoquinone and ethanediamine under ambient conditions [92]. The as-synthesized CNDs had massive amino groups (came from ethanediamine) and lysosomal targeting ability, and their fluorescence emission could sensitively respond to the pH in the lysosomes. Moreover, the CNDs were successfully used to monitor the lysosomal pH dynamics during the apoptosis of living cells. Ye et al. fabricated red-emitting CNDs with two-photon fluorescence excitation ability by one-pot hydrothermal method using *p*-phenylenediamine, *o*-phenylenediamine, and dopamine [106]. The CNDs exhibited a broad pH-sensitive range from 1.0 to 9.0 due to the aggregation and disaggregation of the CNDs. Owing to the excellent fluorescence properties and pH-responsive ability, the CNDs could be used as a fluorescent agent to sense and visualize pH fluctuation in cells, tissue, and zebrafish.

Besides, ratiometric probes with more accurate sensing results have also been designed based on CNDs. Nie et al. prepared a ratiometric probe based on CNDs and pH-sensitive fluorescein isothiocyanate (FITC) [10]. Similarly, CNDs with dual emissions located at 475 and 545 nm under single-wavelength excitation were prepared by the one-pot hydrothermal treatment of citric acid and basic fuchsin (Fig. 6) [105]. Taking advantage of the pH sensitivity of the as-obtained CNDs at the two emissions, ratiometric detection of intracellular pH was successfully realized using the CNDs.

3.2.2 CNDs for Intracellular Metal Ion Sensing

Various metal ions are present in the cells. Some of the metal ions are essential for living cells, while others are toxic to the cells [107]. Therefore, the in situ detection of these metal ions is important for the diagnosis of metal ion-related diseases. Up till now, CNDs have been used to detect many kinds of metal ions (such as Zn^{2+}, Al^{3+}, Fe^{3+}, Cu^{2+}, Ag^{+}, and Hg^{2+}) in living cells.

Zinc (Zn), an essential element in the human body, is an indispensable component of many enzymes. Thus, sensitive detection of Zn^{2+} is important to understand these enzyme-related physiological processes. Yang et al. designed Zn^{2+}-passivated CNDs whose fluorescence could be effectively quenched by ethylenediaminetetraacetic acid disodium salt (EDTA) [108]. Moreover, taking advantage of the complexation between Zn^{2+} and EDTA, the fluorescence of the Zn^{2+}-passivated CND/EDTA complex could be recovered by the addition of external Zn^{2+} with a detection of limit (LOD) of 5.1×10^{-7} M, making the system suitable for monitoring the intracellular Zn^{2+} concentration.

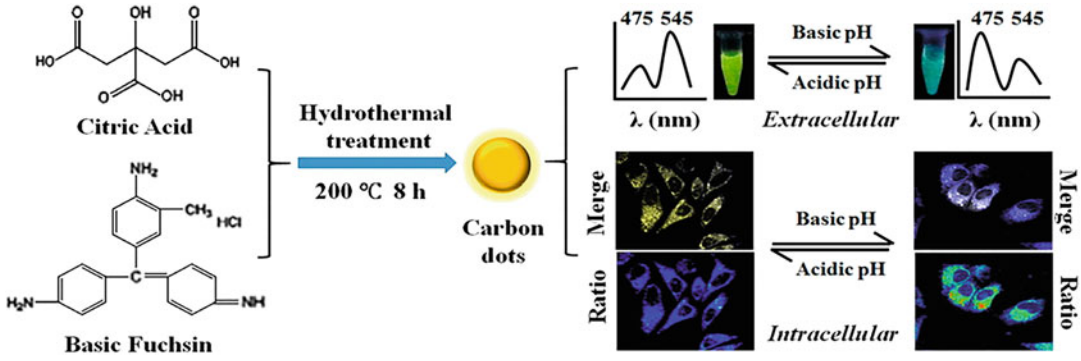

Fig. 6 Schematic illustrating the synthesis of the CNDs (carbon dots) and their application for extracellular and intracellular pH sensing. Reprinted with permission from Ref. [105]. Copyright © 2016 American Chemical Society

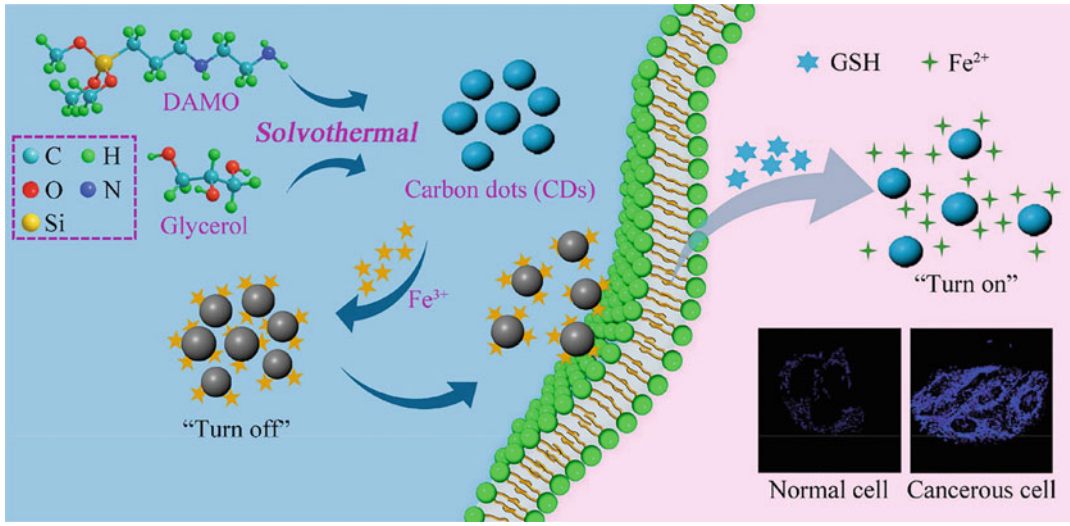

Fig. 7 Schematic illustrating the preparation of the CNDs and their applications for Fe^{3+} detection and cancer/normal cell differentiation. Reprinted with permission from Ref. [115]. Copyright © 2018 Elsevier Ltd. All rights reserved

Al^{3+} ion has been widely investigated in the etiology of neurological disorders, such as Parkinson's disease, Alzheimer's disease, and dialysis encephalopathy [109]. Hence, the accurate detection of Al^{3+} is crucial for understanding the progression of neurological diseases. Kong et al. synthesized amphiphilic blue-emitting CNDs from citric acid and methionine, which could be quenched by morin (MR) through electrostatic interaction [109]. After the addition of Al^{3+}, the system could emit strong green emission due to the Förster resonance energy transfer (FRET) process between the CNDs and the MR-Al^{3+} complex. Besides, the designed system could be used to visualize the Al^{3+} distribution in human umbilical vein endothelial cells.

Ferric ion (Fe^{3+}) can regulate cellular metabolism and oxygen transport in hemoglobin in the human body. The fluorescence of many CNDs shows excellent responsiveness to Fe^{3+} [110–115]. For example, it was reported that the N-doped CNDs derived from a popular antibiotic aminosalicylic acid showed excellent sensitivity to Fe^{3+} in living cells [113]. Similarly, a CND-based fluorescent probe with the "on-off-on" property was fabricated by our group via a one-pot solvothermal method using glycerol and *N*-[3-(trimethoxysilyl)propyl]ethylenediamine (DAMO) as the raw materials (Fig. 7) [115]. The fluorescence of CNDs could be selectively and sensitively quenched by Fe^{3+} with a low LOD of 16 nM. The potential Fe^{3+} detection mechanism of the CNDs was attributed to the presence of the amino groups on the surface of the CNDs. The amino groups may have strong interaction with Fe^{3+}, making the electrons in the excited state transfer to Fe^{3+} and quenching the fluorescence of CNDs.

Besides Fe^{3+} ions, Cu^{2+} ions also play essential structural roles in many proteins and enzymes and are involved in many physiological behaviors. However, high concentrations of intracellular Cu^{2+} are toxic to organisms. To detect the Cu^{2+} concentration in the cells, Salinas-Castillo et al. developed a microwave-assisted strategy to prepare the CNDs with both down- and up-conversion fluorescence properties using citric acid and polyethylenimine as the precursors [116]. The CNDs showed low cytotoxicity and were successfully used for imaging intracellular Cu^{2+} with high selectivity and sensitivity.

Silver has a long and intriguing history as an antibiotic for fighting against bacterial infections, but high concentrations of Ag^{+} can elicit high toxicity [117]. Therefore, sensitive detection of Ag^{+} is highly required. Zuo et al. prepared

fluorine (F)-doped CNDs using 4,5-difluoro-1,2-benzenediamine and tartaric acid as the raw materials, and found that the F-doped CNDs could selectively bind to Ag^+, making the F-doped CNDs suitable for the detection of Ag^+ in various biological systems including mammalian cells [118].

Hg^{2+} as one of the most hazardous and toxic ions to the environment and human health is responsible for many fatal diseases such as nervous system damage and nephritic syndrome even at a low concentration of 2 mg/kg per day [119]. To detect the intracellular Hg^{2+}, two kinds of CNDs were prepared using "citric acid + 1,2-ethylenediamine" and "citric acid + *N*-(*β*-aminoethyl)-*γ*-aminopropyl methyldimethoxysilane (AEAPMS)" as the starting materials [120]. Both of the two types of the CNDs could be effectively quenched by Hg^{2+}, and even trace the Hg^{2+} in living cells. The excellent Hg^{2+} detection selectivity of the CNDs was possibly due to the fact that Hg^{2+} ions have a stronger affinity for the electron-rich surface (due to the presence of amino and carboxyl groups) of the CNDs than other metal ions.

Besides the above-mentioned metal ions, CNDs have also been used to detect other ions, such as Fe^{2+} [121], Sn^{2+} [122], Sn^{4+} [123], Mo^{6+} [123], Pb^{2+} [124], Cr^{6+} [125], and even anions, including I^- [126] and phosphate [127]. However, only a few studies have reported that the CNDs can be used for detecting these ions in the presence of cells or in physiological conditions. In the future, the feasibility of using CNDs for in vitro and in vivo ion detection should be extensively investigated.

3.2.3 CNDs for Intracellular Molecule Sensing

Besides pH and metal ions, CNDs are also a powerful tool for the detection of intracellular molecules. As fluorescent probes, CNDs can detect and image molecules through "turn-off", "on-off-on", and ratiometric ways.

Hydrogen peroxide (H_2O_2) is a prominent member of the reactive oxygen species (ROS) family and necessary in biological systems, and hence the detection of H_2O_2 and the elucidation of its biological functions have become an important research topic in the biological and medical fields. Du et al. designed a CND-based nanoprobe for detecting mitochondrial H_2O_2 by conjugating the CNDs with TPP and 3-oxo-3′,6′-bis(4,4,5,5-tetra-methyl-1,3,2-dioxaborolan-2-yl)-3*H*-spiro [isobenzofuran-1,9′-xanthene]-6-carboxylic acid (PFl) for mitochondrial targeting and H_2O_2 recognition, respectively, in which the CNDs served as the carrier and the FRET donor [128].

Hydrogen sulfide (H_2S) is an endogenous gaseous signaling compound generated in cells via the enzymatic or non-enzymatic pathway, which can regulate cardiovascular, neuronal, and immune systems [129]. Yu et al. designed a CND-based ratiometric fluorescent probe for intracellular H_2S detection [130]. The blue-emitting CNDs ($em = 425$ nm) were conjugated with green-emitting naphthalimide-azide ($em = 526$ nm). No FRET process occurred between the CNDs and naphthalimide-azide without H_2S. After the addition of H_2S, the naphthalimide-azide could be reduced to an energy acceptor naphthalimide-amine by H_2S. As a result, the fluorescence ratio (I_{526}/I_{425}) increased with increasing H_2S concentrations.

Formaldehyde (FA) is an important intermediate in cellular metabolism in mammals, and is related to Alzheimer's disease, cancer, and other diseases. Thus, to develop approaches for detecting FA with high sensitivity and selectivity in living cells is highly required. To this end, as reported by Liu et al., dexamethasone and 1,2,4,5-tetraaminobenzene (TAB) were used to synthesize the lysosome-targeted CNDs for the ratiometric fluorescence detection of FA (Fig. 8) [93]. The residual *o*-diamino groups in the synthesized CNDs could react quickly and selectively with FA, leading to the ratiometric fluorescence response to FA through altering the intramolecular charge transfer (ICT) process from the amino groups (electron donors) to the carbonyl groups (electron acceptors) of the CNDs. Chen et al. synthesized naphthalimide derivative (ND)-conjugated CNDs for monitoring lysosomal FA, in which the fluorescence intensity of green fluorescent ND ($em = 535$ nm) and blue-

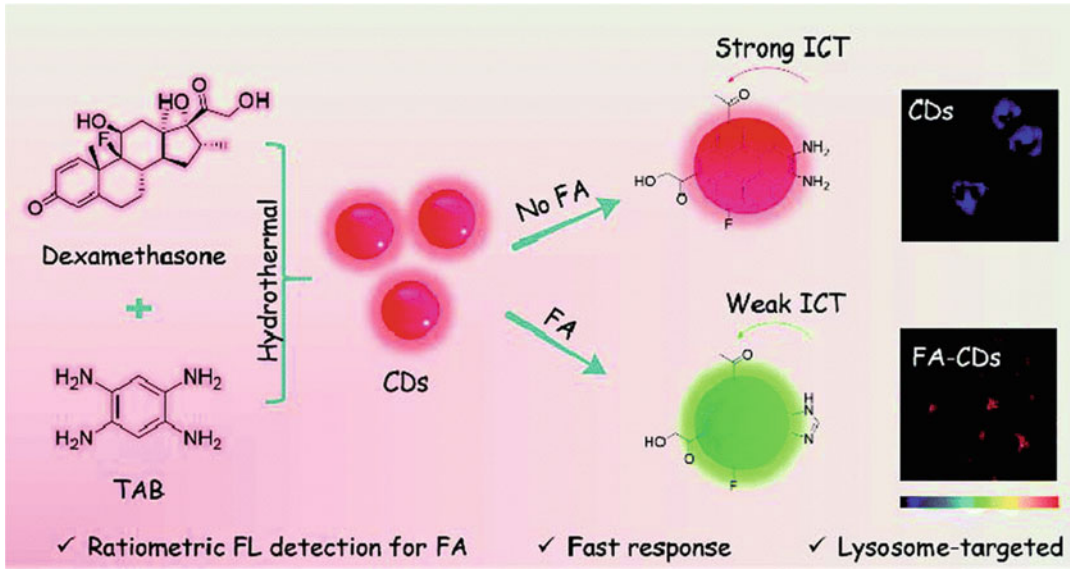

Fig. 8 Schematic illustrating the synthesis of the CNDs (CDs) and their possible mechanism for FA detection. Reprinted with permission from Ref. [93]. Copyright © 2019 Royal Society of Chemistry

fluorescent CNDs ($em = 414$ nm) served as the response signal and the reference signal, respectively [94]. The fluorescence intensity ratio (F_{535}/F_{414}) of the probe was linearly dependent on the FA concentration with a LOD of 3.4×10^{-7} M. Combined with its lysosome-targeting ability, the probe was suitable for the ratiometric fluorescence imaging of FA in lysosomes.

Glutathione (GSH) is an important antioxidant that prevents the cells from being damaged by ROS and heavy metals. Besides, it also participates in many physiological processes such as cell metabolism. As we stated above, our group reported that Fe^{3+} could quench the fluorescence of the CNDs made from glycerol and DAMO [115]. More interestingly, we found that GSH could recover the fluorescence of the CNDs quenched by Fe^{3+}. Based on the different GSH contents in normal cells and cancerous cells [131], we successfully distinguished cancerous cells from normal ones using the mixture of CNDs and Fe^{3+}. Sun et al. also designed an "on-off-on" probe based on the CNDs prepared from citric acid and diethylenetriamine [132]. The fluorescence of the CNDs could be significantly quenched by Hg^{2+}, and could be recovered after the addition of GSH. Then the CND-based fluorescent agent was successfully applied in monitoring the Hg^{2+} and GSH in living cells.

Ascorbic acid (AA), as an essential nutrient for humans, functions as a cofactor in many enzymatic reactions, and is related to many diseases. As a result, to develop a sensitive method for detecting the intracellular AA level is of great importance [133]. Feng et al. prepared near-infrared-emitting CNDs which could be quenched by cobalt oxyhydroxide (CoOOH) nanoflakes by energy transfer [134]. After the addition of AA, CoOOH was reduced to Co^{2+}, resulting in the "turn-on" of the CND fluorescence. The as-prepared nanosystem had high AA detection selectivity and sensitivity with an LOD of 270 nM. Furthermore, the nanosystem was successfully employed for two-photon imaging of endogenous AA in living cells and deep tissues.

Sensitive and selective glucose sensing is highly needed because glucose detection is incredibly important to the patients suffering from diabetes. Kiran et al. found that the boronic acid-functionalized CNDs could enter the cells and form aggregates due to the presence of

glucose in the cells, leading to the fluorescence quenching of the CNDs [135]. As a result, intracellular glucose detection could be realized using the CNDs.

Besides small molecule imaging, CNDs can be used for macromolecule sensing, such as DNA [136] and RNA [137]. Han et al. synthesized carboxyl- and hydroxyl-containing CNDs through acidic oxidation of conductive carbon nanoparticles, and modified the CNDs with *p*-phenylenediamine and 4-carboxybutyl triphenylphosphonium to endow the CNDs with positive charges [138]. Interestingly, the fluorescence intensity of the as-prepared green-emitting CNDs could be enhanced by double-stranded DNA (dsDNA) and single-stranded RNA (ssRNA), and both the absorption and emission profiles of the CNDs had a bathochromic shift after the addition of ssRNA but not dsDNA. Besides, the CNDs could penetrate through various biological barriers, and could emit spectrally distinguishable fluorescence when they bound to dsDNA and ssRNA in living cells, thus realizing real-time visualization of dsDNA and ssRNA in situ.

In addition, CNDs have been successfully used for detecting other molecules such as dopamine [139], tetracycline [140], amino acids [141, 142], and even proteins [143]. Similar to ions, most of these molecules are detected by CNDs without cells. As a result, novel CNDs that are suitable for in vitro and in vivo molecule detection are urgently needed.

3.3 CNDs for Selective Cell Imaging

Owing to their flexibility of surface functionalization, CNDs can be conjugated with targeting motifs for targeted cell imaging. Based on this, Li et al. designed a type of transferrin-modified CNDs for imaging transferrin receptor-overexpressed cancer cells [144]. Wang et al. connected the CNDs with DNA aptamers by carboxyl–amine reaction, and the resultant aptamer-modified CNDs maintained both the bright fluorescence of the CNDs and the recognition ability of the DNA aptamer [18]. The authors also demonstrated that the aptamer-conjugated CNDs could sensitively and selectively image human breast cancer cells (MCF-7 cells).

Besides, it has been reported that some CNDs can selectively image the cells without further modifications. Zheng et al. developed a pyrolysis strategy to synthesize the tumor-targeting CNDs (termed CD-Asp) without the modification of any extra targeting ligands using *D*-glucose and *L*-aspartic acid as the raw materials (the tumor-targeting performance of the CNDs was shown in Fig. 9) [145]. The self-targeting ability of the CNDs was attributed to the presence of *D*-glucose and *L*-aspartic acid residues, which helped the CNDs to cross the blood–brain barrier through the GLUT-1 and ACT2 transporters. Bhunia et al. used tumor-targeting folate molecules as the carbon source to prepare CNDs [146]. The as-prepared CNDs could target folate receptor-overexpressed cancer cells as they expected.

4 CNDs for Microbial Cell Imaging

Microbial infection induced by bacteria, fungi, and viruses is one of the major public health problems worldwide [147]. To fight against microbial infections, early, sensitive, and accurate detection of microorganisms is of great importance. The fluorescence-based methods are considered as a powerful tool for microbial detection. Owing to the outstanding optical properties of CNDs, recent decades have witnessed considerable research progress in their applications in microbial imaging and sensing [148].

Mehta et al. reported the synthesis of *Saccharum officinarum* juice-derived CNDs [149]. The CNDs were proven to be suitable for bacterial and fungal imaging. Nandi et al. synthesized hydrocarbon chain-functionalized amphiphilic CNDs for bacterial detection and imaging [150]. The fluorescence intensity and spectral position of the CNDs were dependent

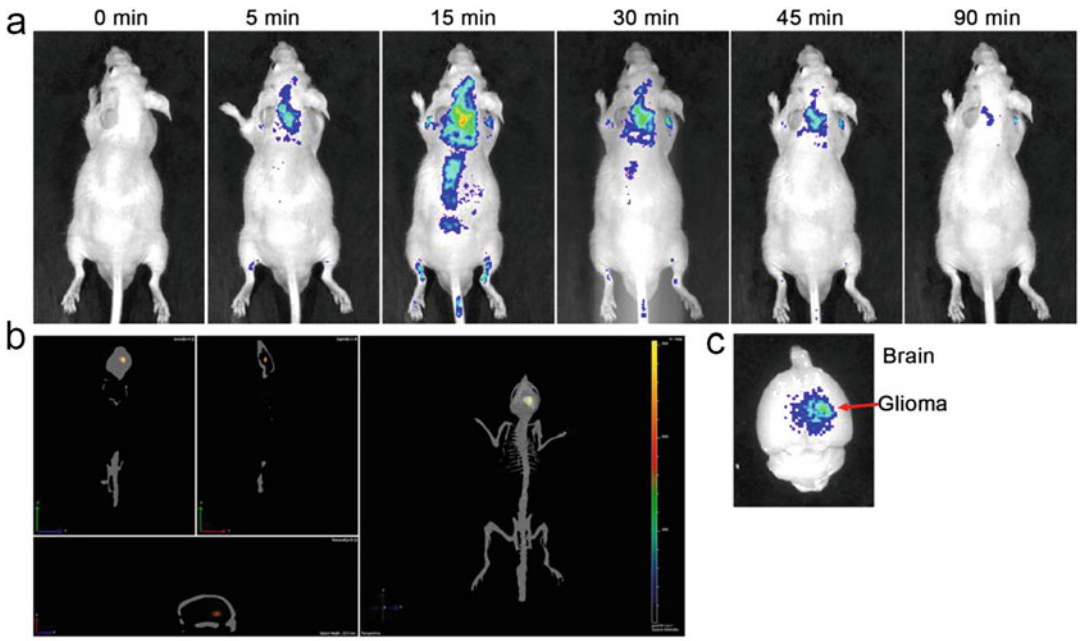

Fig. 9 (**a**) In vivo fluorescence images of C6 glioma-bearing mice after the injection of CD-Asp. (**b**) Three-dimensional reconstruction of CD-Asp distribution in the brain 20 min after injection. (**c**) Ex vivo fluorescence image of the brain 90 min after the injection of CD-Asp. Reprinted with permission from Ref. [145]. Copyright © 2015 American Chemical Society

on the bacterial species, and could be used for distinguishing bacteria.

4.1 CNDs for Gram-Positive and Gram-Negative Bacterial Distinguishment

The Gram staining method is a standard diagnostic method to classify bacteria into Gram-positive and Gram-negative ones. Gram-negative bacteria but not Gram-positive ones are sensitive to some antibiotics such as streptomycin and gentamicin, while Gram-positive bacteria but not Gram-negative ones are sensitive to other antibiotics such as penicillin. Thus, differentiating Gram-positive and Gram-negative bacteria is very important.

Our group prepared quaternized CNDs using the reaction between carboxyl group-containing lauryl betaine and amine group-containing CNDs [151]. The as-synthesized quaternized CNDs (termed CDs-C_{12}) had polarity-sensitive fluorescence emission property, leading to the significantly enhanced fluorescence when the CNDs interacted with the Gram-positive bacteria. Moreover, owing to the presence of both hydrophobic hydrocarbon chains and positively charged quaternary ammonium groups on their surfaces, the CNDs could selectively attach to Gram-positive bacteria (Fig. 10), realizing the bacterial differentiation. Recently, we developed a simpler method for the one-step synthesis of quaternized CNDs via the solvothermal treatment of glycerol and dimethyloctadecyl [3-(trimethoxysilyl)propy]ammonium chloride (termed Si-QAC) [152]. Similarly, the as-obtained CNDs had the bacterial contact-enhanced fluorescence emission property and could be used for fast Gram-type identification.

Besides Gram-positive bacterial imaging, the CNDs have been also used for selective Gram-negative bacterial imaging. Colistin, a well-known antibiotic against Gram-negative bacteria, was reacted with diammonium hydrogen citrate to prepare CNDs [153]. Owing to the excellent specificity of colistin to Gram-negative bacteria, selective imaging of Gram-negative bacteria over

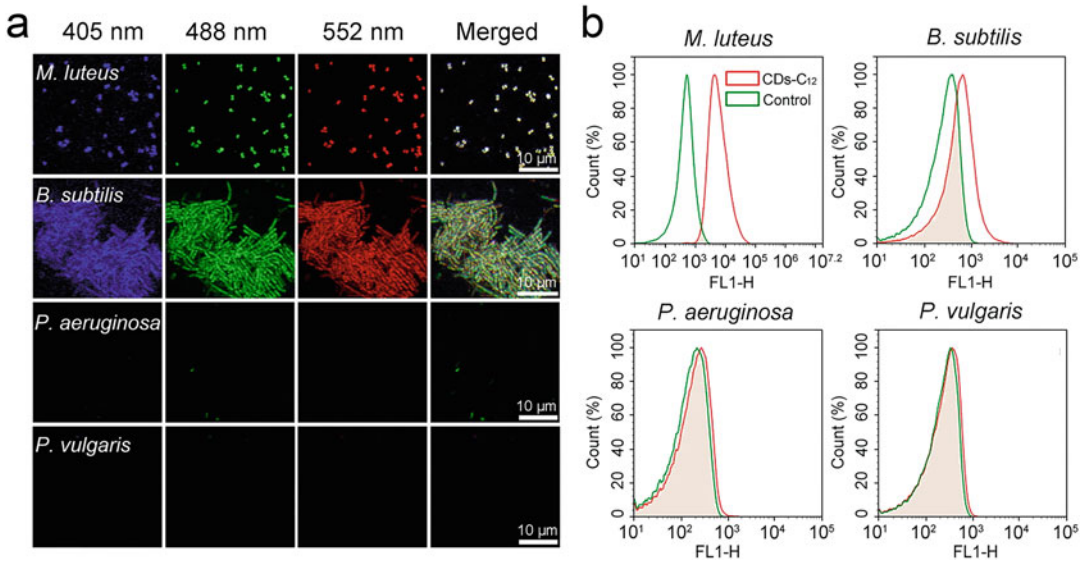

Fig. 10 (**a**) Confocal microscopic images of Gram-positive bacteria (*Micrococcus luteus* (*M. Luteus*) and *Bacillus subtilis* (*B. subtilis*)) and Gram-negative bacteria (*Pseudomonas aeruginosa* (*P. aeruginosa*) and *Proteus vulgaris* (*P. vulgaris*)) after incubation with the quaternized CNDs (CDs-C_{12}) for 1 h under 405, 488, and 552 nm laser excitations. (**b**) Corresponding flow cytometric data. Reprinted with permission from Ref. [151]. Copyright © 2016 American Chemical Society

Gram-positive ones was realized using the CNDs. Similarly, amikacin, an antibiotic with strong bactericidal activity against most Gram-negative bacteria, and diammonium hydrogen citrate were used to prepare CNDs [154]. The amikacin-functionalized CNDs were successfully used for the selective detection of Gram-negative bacteria with an LOD of 552 colony forming units (CFU)/mL.

4.2 CNDs for Microbial Live/Dead Differentiation

To assess the microbial inactivation performance of antimicrobial agents, the distinguishment between live and dead microbial cells is of great importance. Thus, various methods and techniques have been developed for microbial live/dead differentiation, such as the plate counting method, atomic force microscopy, and fluorescence-based methods. Among them, the fluorescence labeling method is one of the most commonly used approaches for rapidly and sensitively distinguishing live/dead microbial cells [155].

Our group prepared bacteria-derived CNDs with a highly negative zeta potential of −42 mV [29]. The CNDs were hard to be internalized by live bacterial cells due to the strong electrostatic repulsion between the CNDs and the bacterial surfaces, but could enter the dead cells with damaged cell surfaces. As a result, the CNDs could selectively image the dead microbial cells (Fig. 11). Compared to propidium iodide (PI) which is a commercial dye for dead cell imaging, the as-synthesized CNDs showed low toxicity to microbial cells and excellent photostability. Nitrogen- and phosphorus-doped CNDs with tunable surface potentials were prepared using a facile hydrothermal method [156]. Similarly, the obtained CNDs selectively stained dead bacterial cells but not live ones due to the electrostatic repulsion between the negatively charged CNDs and the negatively charged bacterial walls.

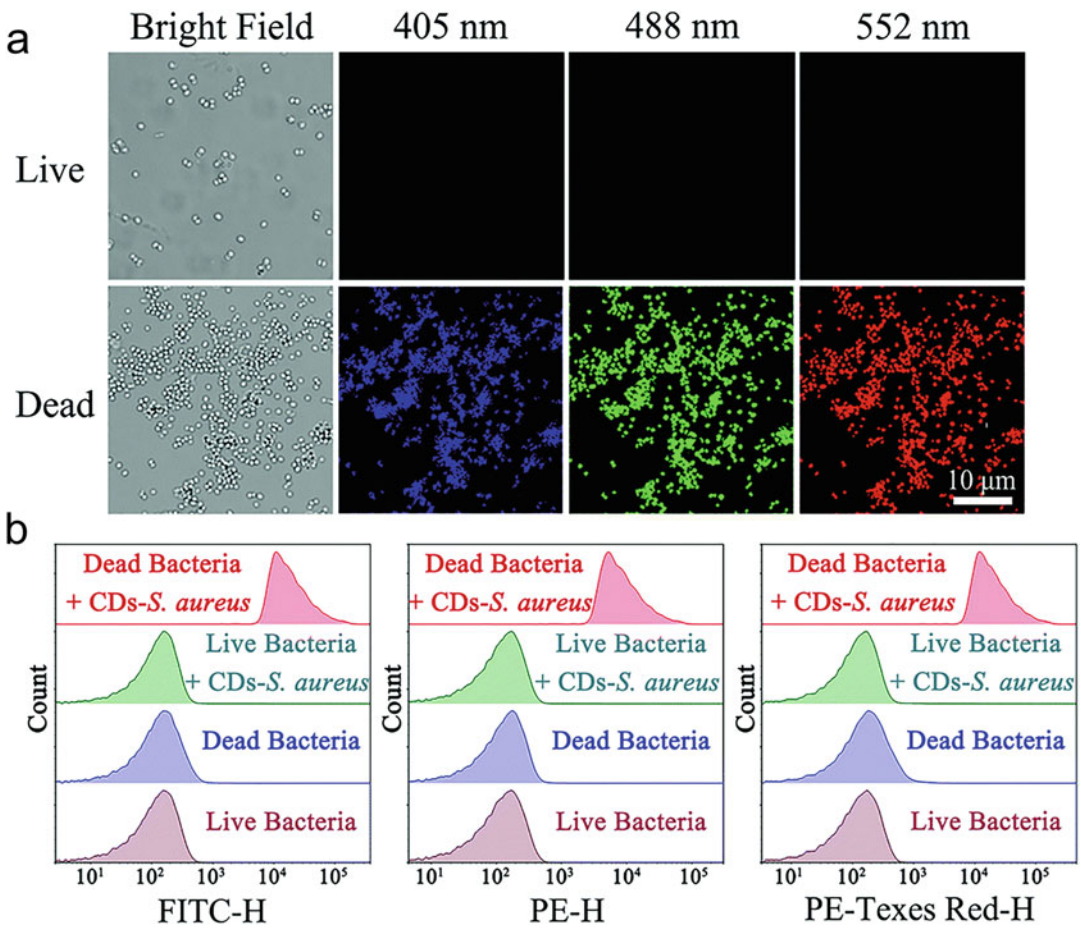

Fig. 11 Confocal microscopic images (**a**) and flow cytometric results (**b**) of live and dead *S. aureus* stained with the CNDs (CDs-*S. aureus*) for 1 h. Reprinted with permission from Ref. [29]. Copyright © 2017 Royal Society of Chemistry

4.3 CNDs for Microbial Biofilm Imaging

Microbial biofilms are surface-attached communities of microbes encased in an extracellular matrix of biomolecules and display high levels of antibiotic tolerance, because most antibiotics cannot penetrate the biofilms effectively [157]. Similar to antibacterial agents, fluorescent materials could also be blocked by the sticky extracellular polymeric substance (EPS) matrix, which hinders their successful biofilm imaging.

Ritenberg et al. showed that the amphiphilic CNDs could readily bind to the EPS scaffold of the bacteria *P. aeruginosa*, making them suitable for the fluorescence microscopic visualization of the EPS structural features [158]. Lin et al. developed a one-step hydrothermal carbonization method to synthesize the CNDs from the bacteria *Lactobacillus plantarum* (*L. plantarum*) [30]. The as-prepared CNDs were found to be capable of imaging the microorganisms within the biofilms. Our group prepared Si-QAC/glycerol-derived CNDs by a solvothermal method [152] and used the obtained CNDs with ultrasmall size (~3.3 nm) and strong positively charged surfaces (zeta

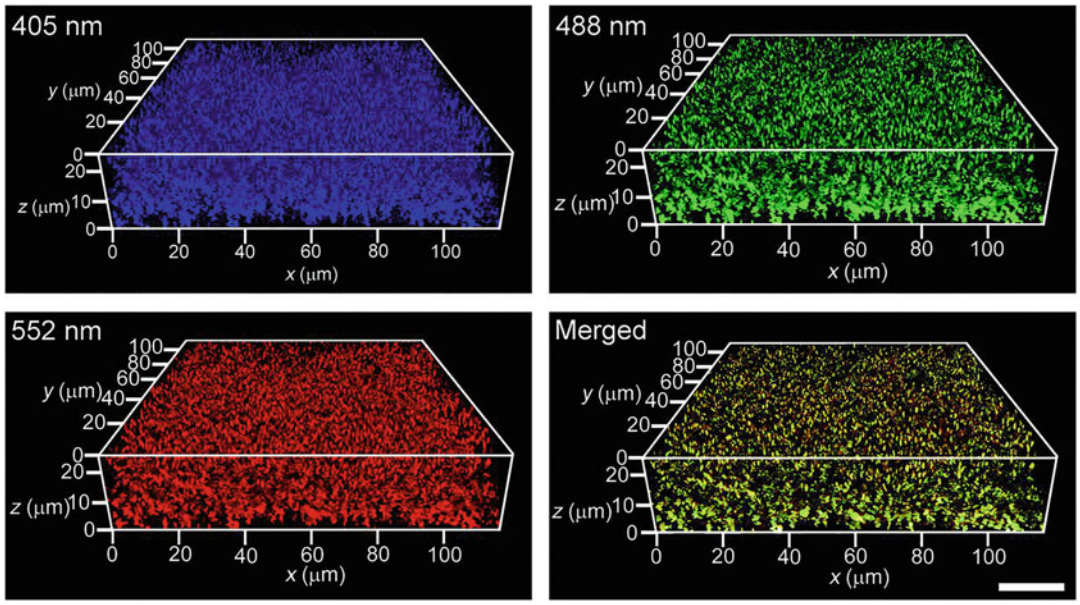

Fig. 12 Three-dimensional confocal microscopic images of an *S. aureus* biofilm stained with the CNDs (Si-QAC CDs). These images include the ones taken under different excitation wavelengths and the merged one. Reprinted with permission from Ref. [159]. Copyright © 2019 Royal Society of Chemistry

potential: ~33 mV) for excellent fluorescence imaging of the *S. aureus* biofilms [159] (Fig. 12).

As stated above, CNDs have become a powerful tool for microbial imaging, including Gram-positive and Gram-negative bacterial distinguishment, microbial live/dead differentiation, and biofilm imaging. Although many studies have demonstrated that CNDs can image bacteria and fungi, few studies have reported virus imaging using CNDs. Besides, taking advantage of the excellent optical properties of CNDs and super-resolution fluorescence imaging techniques [151, 160], the imaging of subcellular structures in microbial cells may also be realized; however, relevant studies are still lacking.

5 CNDs for Plant Cell Imaging

Besides mammalian and microbial cells, CNDs also show potential in imaging plant cells. CNDs usually have ultrasmall sizes, enabling their penetration into the walls and membranes of the plant cells.

Zhang et al. found that the chiral CNDs fabricated from *D*-cysteine and citric acid could be absorbed by mung beans during the period of seed germination, and were detected in the vascular system of the root, stem, and leaf after 5-day incubation [161]. Wang et al. synthesized bright CNDs using *L*-glutamic acid with nitric acid as a carbonization agent and ethylene glycol as a passivation agent [162]. The CNDs with negligible cytotoxicity could be endocytosed by intact plant cells with 10 min and even directly stain the nuclei of these cells (Fig. 13). Li et al. found that the CNDs prepared from *p*-phenylenediamine have a strong affinity for cellulose through hydrogen bonding, and the PLQY of the CNDs dramatically increased from 8% to 44% when the CNDs were dispersed in cellulose matrices [163]. The authors demonstrated that the affinity of the CNDs for binding cellulose endowed them with the capability of imaging the cellulosic plant cell walls.

Recent studies have reported that some CNDs are able to enhance the production of cereal crops [164] and promote carbohydrate accumulation in

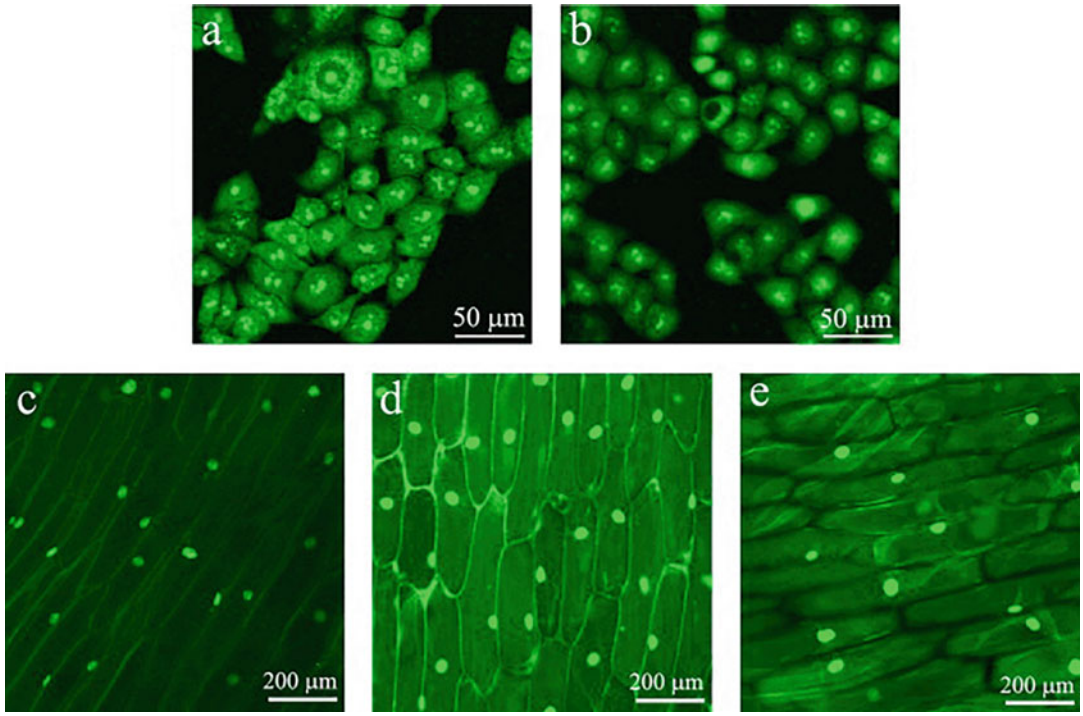

Fig. 13 Confocal microscopic images of HeLa cells incubated with CNDs (**a**) and acridine orange (AO) (**b**), and onion epidermal cells incubated with CNDs for 10 and 60 min (**c**, **d**) and AO (**e**). Reprinted with permission from Ref. [162]. Copyright © 2014 Elsevier Ltd. All rights reserved

mung bean plants [161]. However, the detailed interaction mechanisms between CNDs and plants remain largely unknown. Using CNDs for plant cell imaging will help the researchers to investigate the interactions between CNDs and plants, and study the biodistribution of the CNDs in the plants. Besides, whether the various CNDs synthesized by the researchers can be used for plant cell imaging should be tested to enrich the applications of the CNDs and foster the advancement of the CND-related plant research. Further, to get a deep understanding of the interaction between CNDs and plant cells, the evaluation of the CNDs for organelle-specific imaging in plant cells is highly desirable.

6 Conclusion and Future Perspective

With their ultrasmall size, ease of preparation and modification, good anti-photoblinking and anti-photobleaching properties, and excellent biocompatibility, CNDs have become popular probes for bioimaging. Up to now, CNDs have been successfully used in imaging various cells, including mammalian cells, microbial cells, and plant cells. Subcellular distributions and selective/sensitive detection of ions/molecules using CNDs can be achieved by controlling their size, charge, and surface chemistry.

Although many efforts have been devoted to the preparation of CNDs and cell imaging using CNDs, there are still several issues that need to be addressed in the future. First, most CNDs have broad and excitation-dependent emissions, limiting their imaging applications when they are used in combination with other fluorescent probes. Hence, novel CNDs with bright and narrow emissions are highly desired. Second, a large number of CNDs with novel optical properties such as two-photon excitation [165–167], long-wavelength emission [168–170], room-temperature phosphorescence [50, 171–173],

photo-activation [174], piezochromic luminescence [174–176], up-conversion properties [177–179], and electrochemiluminescence [143], have been synthesized, and their applications in bioimaging also need to be investigated. Third, many CNDs have poor water-dispersity and low cellular uptake efficiency. Thus, developing suitable surface modification strategies for these CNDs is in urgent need for improving their cell imaging performance. Fourth, the structures of most CNDs are not clear, and the mechanisms of the interactions between CNDs and cells, organelles, or intracellular ions/molecules need to be further investigated. It is challenging to rationally design CNDs with suitable compositions, sizes, and surface chemistries for monitoring the cells, organelles, ions, and molecules with high selectivity and sensitivity. Fifth, although CNDs have been used for imaging many organelles (including nuclei, mitochondria, lysosomes, and Golgi apparatus), ions, and molecules, new kinds of CNDs need to be synthesized to image other subcellular structures (such as plasma membrane, cell wall, endoplasmic reticulum, ribosome, centrosome, lipid droplet, and peroxisome) and intracellular ions/molecules. Sixth, owing to their surface modifiability, the diverse CNDs can be conjugated with specific targeting ligands to be ideal probes for imaging various cells (such as cancer cells, inflammation-related cells, stem cells, and immune cells), subcellular structures, and intracellular ions/molecules. Hence, more efforts should be devoted to the modification of the CNDs for realizing the selective imaging of these cells and cellular structures/compositions. Seventh, most of the CNDs can be quenched by the ions/molecules, thus realizing molecule/ion detection. However, the design of CND-based "turn-on" probes for intracellular ion/molecule imaging is still lacking. Eighth, recent studies regarding the use of CNDs for bioimaging mainly focus on mammalian cell imaging, but the applications of CNDs in microbial cells and plant cells are still insufficient. The imaging performance of the developed CNDs for microbial and plant cell imaging should be extensively evaluated. Last, due to their excellent optical properties and good biocompatibility, CNDs may have potential in the selective imaging of cellular biomacromolecules such as the protein antigens on the cell surfaces. The feasibility of using CNDs for monitoring the biomacromolecules should be tested.

References

1. Li XM, Rui MC, Song JZ, Shen ZH, Zeng HB (2015) Carbon and graphene quantum dots for optoelectronic and energy devices: a review. Adv Funct Mater 25:4929–4947
2. Zhu SJ, Song YB, Zhao XH, Shao JR, Zhang JH, Yang B (2015). The photoluminescence mechanism in carbon dots (graphene quantum dots, carbon nanodots, and polymer dots): current state and future perspective. Nano Res 8:355–381
3. Meng WX, Bai X, Wang BY, Liu ZY, Lu SY, Yang B (2019) Biomass-derived carbon dots and their applications. Energy Environ Mater 2:172–192
4. Xu XY, Ray R, Gu YL, Ploehn HJ, Gearheart L, Raker K, Scrivens WA (2004) Electrophoretic analysis and purification of fluorescent single-walled carbon nanotube fragments. J Am Chem Soc 126:12736–12737
5. Sun YP, Zhou B, Lin Y, Wang W, Fernando KAS, Pathak P, Meziani MJ, Harruff BA, Wang X, Wang HF, Luo PJG, Yang H, Kose ME, Chen BL, Veca LM, Xie SY (2006) Quantum-sized carbon dots for bright and colorful photoluminescence. J Am Chem Soc 128:7756–7757
6. Bao L, Zhang ZL, Tian ZQ, Zhang L, Liu C, Lin Y, Qi BP, Pang DW (2011) Electrochemical tuning of luminescent carbon nanodots: from preparation to luminescence mechanism. Adv Mater 23:5801–5806
7. Zheng HZ, Wang QL, Long YJ, Zhang HJ, Huang XX, Zhu R (2011) Enhancing the luminescence of carbon dots with a reduction pathway. Chem Commun 47:10650–10652
8. Yang JJ, Gao G, Zhang XD, Ma YH, Jia HR, Jiang YW, Wang ZF, Wu FG (2017) Ultrasmall and photostable nanotheranostic agents based on carbon quantum dots passivated with polyamine-containing organosilane molecules. Nanoscale 9:15441–15452
9. Xu D, Lin Q, Chang HT (2020) Recent advances and sensing applications of carbon dots. Small Methods 4 (4):1900387
10. Nie H, Li MJ, Li QS, Liang SJ, Tan YY, Sheng L, Shi W, Zhang SXA (2014) Carbon dots with continuously tunable full-color emission and their application in ratiometric pH sensing. Chem Mater 26:3104–3112
11. Pan LL, Sun S, Zhang AD, Jiang K, Zhang L, Dong CQ, Huang Q, Wu AG, Lin HW (2015) Truly fluorescent excitation-dependent carbon dots and their

applications in multicolor cellular imaging and multidimensional sensing. Adv Mater 27:7782–7787
12. Sharma A, Gadly T, Gupta A, Ballal A, Ghosh SK, Kumbhakar M (2016) Origin of excitation dependent fluorescence in carbon nanodots. J Phys Chem Lett 7:3695–3702
13. van Dam B, Nie H, Ju B, Marino E, Paulusse JMJ, Schall P, Li MJ, Dohnalova K (2017) Excitation-dependent photoluminescence from single-carbon dots. Small 13:1702098
14. Wang CX, Xu ZZ, Cheng H, Lin HH, Humphrey MG, Zhang C (2015) A hydrothermal route to water-stable luminescent carbon dots as nanosensors for pH and temperature. Carbon 82:87–95
15. Wang N, Wang YT, Guo TT, Yang T, Chen ML, Wang JH (2016) Green preparation of carbon dots with papaya as carbon source for effective fluorescent sensing of Iron (III) and Escherichia coli. Biosens Bioelectron 85:68–75
16. Fan YZ, Zhang Y, Li N, Liu SG, Liu T, Li NB, Luo HQ (2017) A facile synthesis of water-soluble carbon dots as a label-free fluorescent probe for rapid, selective and sensitive detection of picric acid. Sens Actuators B Chem 240:949–955
17. Li SH, Amat D, Peng ZL, Vanni S, Raskin S, De Angulo G, Othman AM, Grahamb RM, Leblanc RM (2016) Transferrin conjugated nontoxic carbon dots for doxorubicin delivery to target pediatric brain tumor cells. Nanoscale 8:16662–16669
18. Wang ZG, Fu BS, Zou SW, Duan B, Chang CY, Yang B, Zhou X, Zhang LN (2016) Facile construction of carbon dots via acid catalytic hydrothermal method and their application for target imaging of cancer cells. Nano Res 9:214–223
19. Feng T, Ai XZ, An GH, Yang PP, Zhao YL (2016) Charge-convertible carbon dots for imaging-guided drug delivery with enhanced in vivo cancer therapeutic efficiency. ACS Nano 10:4410–4420
20. Liu Q, Guo BD, Rao ZY, Zhang BH, Gong JR (2013) Strong two-photon-induced fluorescence from photostable, biocompatible nitrogen-doped graphene quantum dots for cellular and deep-tissue imaging. Nano Lett 13:2436–2441
21. Liu YB, Zhou L, Li YN, Deng RP, Zhang HJ (2017) Highly fluorescent nitrogen-doped carbon dots with excellent thermal and photo stability applied as invisible ink for loading important information and anti-counterfeiting. Nanoscale 9:491–496
22. Sun MH, Liang C, Tian Z, Ushakova EV, Li D, Xing GC, Qu SN, Rogach AL (2019) Realization of the photostable intrinsic core emission from carbon dots through surface deoxidation by ultraviolet irradiation. J Phys Chem Lett 10:3094–3100
23. Huang YF, Zhou X, Zhou R, Zhang H, Kang KB, Zhao M, Peng Y, Wang Q, Zhang HL, Qiu WY (2014) One-pot synthesis of highly luminescent carbon quantum dots and their nontoxic ingestion by zebrafish for in vivo imaging. Chem Eur J 20:5640–5648
24. Zhu SJ, Meng QN, Wang L, Zhang JH, Song YB, Jin H, Zhang K, Sun HC, Wang HY, Yang B (2013) Highly photoluminescent carbon dots for multicolor patterning, sensors, and bioimaging. Angew Chem Int Ed 52:3953–3957
25. Xu Q, Pu P, Zhao JG, Dong CB, Gao C, Chen YS, Chen JR, Liu Y, Zhou HJ (2015) Preparation of highly photoluminescent sulfur-doped carbon dots for Fe(III) detection. J Mater Chem A 3:542–546
26. Zhang Z, Hao JH, Zhang J, Zhang BL, Tang JL (2012) Protein as the source for synthesizing fluorescent carbon dots by a one-pot hydrothermal route. RSC Adv 2:8599–8601
27. Ge JC, Jia QY, Liu WM, Guo L, Liu QY, Lan MH, Zhang HY, Meng XM, Wang PF (2015) Red-emissive carbon dots for fluorescent, photoacoustic, and thermal theranostics in living mice. Adv Mater 27:4169–4177
28. Hu SL, Wei ZJ, Chang Q, Trinchi A, Yang JL (2016) A facile and green method towards coal-based fluorescent carbon dots with photocatalytic activity. Appl Surf Sci 378:402–407
29. Hua XW, Bao YW, Wang HY, Chen Z, Wu FG (2017) Bacteria-derived fluorescent carbon dots for microbial live/dead differentiation. Nanoscale 9:2150–2161
30. Lin FM, Li CC, Dong L, Fu DG, Chen Z (2017) Imaging biofilm-encased microorganisms using carbon dots derived from L. plantarum. Nanoscale 9:9056–9064
31. Zheng XT, Ananthanarayanan A, Luo KQ, Chen P (2015) Glowing graphene quantum dots and carbon dots: properties, syntheses, and biological applications. Small 11:1620–1636
32. Peng H, Li Y, Jiang CL, Luo CH, Qi RJ, Huang R, Duan CG, Travas-Sejdic J (2016) Tuning the properties of luminescent nitrogen-doped carbon dots by reaction precursors. Carbon 100:386–394
33. Jiang K, Sun S, Zhang L, Lu Y, Wu AG, Cai CZ, Lin HW (2015) Red, green, and blue luminescence by carbon dots: full-color emission tuning and multicolor cellular imaging. Angew Chem Int Ed 54:5360–5363
34. Zhang CF, Hu ZB, Song L, Cui YY, Liu XF (2015) Valine-derived carbon dots with colour-tunable fluorescence for the detection of Hg^{2+} with high sensitivity and selectivity. New J Chem 39:6201–6206
35. Hutton GAM, Martindale BCM, Reisner E (2017) Carbon dots as photosensitisers for solar-driven catalysis. Chem Soc Rev 46:6111–6123
36. Semeniuk M, Yi ZH, Poursorkhabi V, Tjong J, Jaffer S, Lu ZH, Sain M (2019) Future perspectives and review on organic carbon dots in electronic applications. ACS Nano 13:6224–6255
37. Li MX, Chen T, Gooding JJ, Liu JQ (2019) Review of carbon and graphene quantum dots for sensing. ACS Sens 4:1732–1748

38. Mishra V, Patil A, Thakur S, Kesharwani P (2018) Carbon dots: emerging theranostic nanoarchitectures. Drug Discov Today 23:1219–1232
39. Sharma V, Tiwari P, Mobin SM (2017) Sustainable carbon-dots: recent advances in green carbon dots for sensing and bioimaging. J Mater Chem B 5:8904–8924
40. Li HX, Yan X, Kong DS, Jin R, Sun CY, Du D, Lin YH, Lu GY (2020) Recent advances in carbon dots for bioimaging applications. Nanoscale Horiz 5:218–234
41. Wang W, Cheng L, Liu WG (2014) Biological applications of carbon dots. Sci China Chem 57:522–539
42. Song YB, Zhu SJ, Yang B (2014) Bioimaging based on fluorescent carbon dots. RSC Adv 4:27184–27200
43. Liu X, Pang JH, Xu F, Zhang XM (2016) Simple approach to synthesize amino-functionalized carbon dots by carbonization of chitosan. Sci Rep 6:31100
44. Zhang YQ, Ma DK, Zhuang Y, Zhang X, Chen W, Hong LL, Yan QX, Yu K, Huang SM (2012) One-pot synthesis of N-doped carbon dots with tunable luminescence properties. J Mater Chem 22:16714–16718
45. Li XM, Zhang SL, Kulinich SA, Liu YL, Zeng HB (2014) Engineering surface states of carbon dots to achieve controllable luminescence for solid-luminescent composites and sensitive Be^{2+} detection. Sci Rep 4:4976
46. Vedamalai M, Periasamy AP, Wang CW, Tseng YT, Ho LC, Shih CC, Chang HT (2014) Carbon nanodots prepared from o-phenylenediamine for sensing of Cu^{2+} ions in cells. Nanoscale 6:13119–13125
47. Zhang XD, Chen XK, Kai SQ, Wang HY, Yang JJ, Wu FG, Chen Z (2015) Highly sensitive and selective detection of dopamine using one-pot synthesized highly photoluminescent silicon nanoparticles. Anal Chem 87:3360–3365
48. Wu FG, Zhang XD, Kai SQ, Zhang MY, Wang HY, Myers JN, Weng YX, Liu PD, Gu N, Chen Z (2015) One-step synthesis of superbright water-soluble silicon nanoparticles with photoluminescence quantum yield exceeding 80%. Adv Mater Interfaces 2:1500360
49. Zhang YQ, Liu XY, Fan Y, Guo XY, Zhou L, Lv Y, Lin J (2016) One-step microwave synthesis of N-doped hydroxyl-functionalized carbon dots with ultra-high fluorescence quantum yields. Nanoscale 8:15281–15287
50. Jiang K, Wang YH, Gao XL, Cai CZ, Lin HW (2018) Facile, quick, and gram-scale synthesis of ultralong-lifetime room-temperature-phosphorescent carbon dots by microwave irradiation. Angew Chem Int Ed 57:6216–6220
51. Gao G, Jiang YW, Yang JJ, Wu FG (2017) Mitochondria-targetable carbon quantum dots for differentiating cancerous cells from normal cells. Nanoscale 9:18368–18378
52. Li HT, Ming H, Liu Y, Yu H, He XD, Huang H, Pan KM, Kang ZH, Lee ST (2011) Fluorescent carbon nanoparticles: electrochemical synthesis and their pH sensitive photoluminescence properties. New J Chem 35:2666–2670
53. Hou YX, Lu QJ, Deng JH, Li HT, Zhang YY (2015) One-pot electrochemical synthesis of functionalized fluorescent carbon dots and their selective sensing for mercury ion. Anal Chim Acta 866:69–74
54. Deng JH, Lu QJ, Mi NX, Li HT, Liu ML, Xu MC, Tan L, Xie QJ, Zhang YY, Yao SZ (2014) Electrochemical synthesis of carbon nanodots directly from alcohols. Chem Eur J 20:4993–4999
55. Li HT, He XD, Kang ZH, Huang H, Liu Y, Liu JL, Lian SY, Tsang CHA, Yang XB, Lee ST (2010) Water-soluble fluorescent carbon quantum dots and photocatalyst design. Angew Chem Int Ed 49:4430–4434
56. Li Y, Hu Y, Zhao Y, Shi GQ, Deng LE, Hou YB, Qu LT (2011) An electrochemical avenue to green-luminescent graphene quantum dots as potential electron-acceptors for photovoltaics. Adv Mater 23:776–780
57. Lu J, Yang JX, Wang JZ, Lim AL, Wang S, Loh KP (2009) One-pot synthesis of fluorescent carbon nanoribbons, nanoparticles, and graphene by the exfoliation of graphite in ionic liquids. ACS Nano 3:2367–2375
58. Li Y, Zhao Y, Cheng HH, Hu Y, Shi GQ, Dai LM, Qu LT (2012) Nitrogen-doped graphene quantum dots with oxygen-rich functional groups. J Am Chem Soc 134:15–18
59. Ananthanarayanan A, Wang XW, Routh P, Sana B, Lim S, Kim DH, Lim KH, Li J, Chen P (2014) Facile synthesis of graphene quantum dots from 3D graphene and their application for Fe^{3+} sensing. Adv Funct Mater 24:3021–3026
60. Peng J, Gao W, Gupta BK, Liu Z, Romero-Aburto R, Ge LH, Song L, Alemany LB, Zhan XB, Gao GH (2012) Graphene quantum dots derived from carbon fibers. Nano Lett 12:844–849
61. Shinde DB, Pillai VK (2012) Electrochemical preparation of luminescent graphene quantum dots from multiwalled carbon nanotubes. Chem Eur J 18:12522–12528
62. Zhang XY, Wang SQ, Zhu CY, Liu MY, Ji Y, Feng L, Tao L, Wei Y (2013) Carbon-dots derived from nanodiamond: photoluminescence tunable nanoparticles for cell imaging. J Colloid Interface Sci 397:39–44
63. Wang QL, Zheng HZ, Long YJ, Zhang LY, Gao M, Bai WJ (2011) Microwave–hydrothermal synthesis of fluorescent carbon dots from graphite oxide. Carbon 49:3134–3140
64. Tan MQ, Zhang LX, Tang R, Song XJ, Li YM, Wu H, Wang YF, Lv GJ, Liu WF, Ma XJ (2013) Enhanced photoluminescence and characterization of multicolor carbon dots using plant soot as a carbon source. Talanta 115:950–956
65. Hu C, Yu C, Li MY, Wang XN, Yang JY, Zhao ZB, Eychmüller A, Sun YP, Qiu JS (2014) Chemically

tailoring coal to fluorescent carbon dots with tuned size and their capacity for Cu (II) detection. Small 10:4926–4933
66. Dong YQ, Chen CQ, Zheng XT, Gao LL, Cui ZM, Yang HB, Guo CX, Chi YW, Li CM (2012) One-step and high yield simultaneous preparation of single- and multi-layer graphene quantum dots from CX-72 carbon black. J Mater Chem 22:8764–8766
67. Qiao ZA, Wang YF, Gao Y, Li HW, Dai TY, Liu YL, Huo QS (2010) Commercially activated carbon as the source for producing multicolor photoluminescent carbon dots by chemical oxidation. Chem Commun 46:8812–8814
68. Lai CW, Hsiao YH, Peng YK, Chou PT (2012) Facile synthesis of highly emissive carbon dots from pyrolysis of glycerol; gram scale production of carbon dots/mSiO$_2$ for cell imaging and drug release. J Mater Chem 22:14403–14409
69. Mehta VN, Jha S, Singhal RK, Kailasa SK (2014) Preparation of multicolor emitting carbon dots for HeLa cell imaging. New J Chem 38:6152–6160
70. Feng J, Wang WJ, Hai X, Yu YL, Wang JH (2016) Green preparation of nitrogen-doped carbon dots derived from silkworm chrysalis for cell imaging. J Mater Chem B 4:387–393
71. Ding P, Wang HY, Song B, Ji XY, Su YY, He Y (2017) In situ live-cell nucleus fluorescence labeling with bioinspired fluorescent probes. Anal Chem 89:7861–7868
72. Li D, Qiao ZZ, Yu YR, Tang JL, He XX, Shi H, Ye XS, Lei YL, Wang KM (2018) In situ fluorescence activation of DNA–silver nanoclusters as a label-free and general strategy for cell nucleus imaging. Chem Commun 54:1089–1092
73. Chen XK, Zhang XD, Guo YX, Zhu YX, Liu XY, Chen Z, Wu FG (2019) Smart supramolecular "Trojan horse"-inspired nanogels for realizing light-triggered nuclear drug influx in drug-resistant cancer cells. Adv Funct Mater 29:1807772
74. Yang L, Jiang WH, Qiu LP, Jiang XW, Zuo DY, Wang DK, Yang L (2015) One pot synthesis of highly luminescent polyethylene glycol anchored carbon dots functionalized with a nuclear localization signal peptide for cell nucleus imaging. Nanoscale 7:6104–6113
75. Jung YK, Shin E, Kim BS (2015) Cell nucleus-targeting zwitterionic carbon dots. Sci Rep 5:18807
76. Ci JL, Tian Y, Kuga S, Niu ZW, Wu M, Huang Y (2017) One-pot green synthesis of nitrogen-doped carbon quantum dots for cell nucleus labeling and copper (II) detection. Chem Asian J 12:2916–2921
77. Boisvert FM, van Koningsbruggen S, Navascués J, Lamond AI (2007) The multifunctional nucleolus. Nat Rev Mol Cell Biol 8:574–585
78. Frottin F, Schueder F, Tiwary S, Gupta R, Körner R, Schlichthaerle T, Cox J, Jungmann R, Hartl F, Hipp M (2019) The nucleolus functions as a phase-separated protein quality control compartment. Science 365:342–347
79. Barbosa CDES, Corrêa JR, Medeiros GA, Barreto G, Magalhães KG, de Oliveira AL, Spencer J, Rodrigues MO, Neto BAD (2015) Carbon dots (C-dots) from cow manure with impressive subcellular selectivity tuned by simple chemical modification. Chem Eur J 21:5055–5060
80. Kong WQ, Liu RH, Li H, Liu J, Huang H, Liu Y, Kang ZH (2014) High-bright fluorescent carbon dots and their application in selective nucleoli staining. J Mater Chem B 2:5077–5082
81. Hua XW, Bao YW, Wu FG (2018) Fluorescent carbon quantum dots with intrinsic nucleolus-targeting capability for nucleolus imaging and enhanced cytosolic and nuclear drug delivery. ACS Appl Mater Interfaces 10:10664–10677
82. Hua XW, Bao YW, Zeng J, Wu FG (2019) Nucleolus-targeted red emissive carbon dots with polarity-sensitive and excitation-independent fluorescence emission: high-resolution cell imaging and in vivo tracking. ACS Appl Mater Interfaces 11:32647–32658
83. McBride HM, Neuspiel M, Wasiak S (2006) Mitochondria: more than just a powerhouse. Curr Biol 16:R551–R560
84. Wang BB, Wang YF, Wu H, Song XJ, Guo X, Zhang DM, Ma XJ, Tan MQ (2014) A mitochondria-targeted fluorescent probe based on TPP-conjugated carbon dots for both one-and two-photon fluorescence cell imaging. RSC Adv 4:49960–49963
85. Hua XW, Bao YW, Chen Z, Wu FG (2017) Carbon quantum dots with intrinsic mitochondrial targeting ability for mitochondria-based theranostics. Nanoscale 9:10948–10960
86. De Duve C, Wattiaux R (1966) Functions of lysosomes. Annu Rev Physiol 28:435–492
87. Chen XK, Zhang XD, Xia LY, Wang HY, Chen Z, Wu FG (2018) One-step synthesis of ultrasmall and ultrabright organosilica nanodots with 100% photoluminescence quantum yield: long-term lysosome imaging in living, fixed, and permeabilized cells. Nano Lett 18:1159–1167
88. Zhang XD, Chen XK, Guo YX, Jia HR, Jiang YW, Wu FG (2020) Endosome/lysosome-detained supramolecular nanogels as an efflux retarder and autophagy inhibitor for repeated photodynamic therapy of multidrug-resistant cancer. Nanoscale Horiz 5:481–487
89. Wu LL, Li XL, Ling YF, Huang CS, Jia NQ (2017) Morpholine derivative-functionalized carbon dots-based fluorescent probe for highly selective lysosomal imaging in living cells. ACS Appl Mater Interfaces 9:28222–28232
90. Zhang DY, Zheng Y, Zhang H, He L, Tan CP, Sun JH, Zhang W, Peng XY, Zhan QQ, Ji LN, Mao ZW (2017) Ruthenium complex-modified carbon nanodots for lysosome-targeted one- and two-photon imaging and photodynamic therapy. Nanoscale 9:18966–18976

91. E S, Mao QX, Yuan XL, Kong XL, Chen XW, Wang JH (2018) Targeted imaging of the lysosome and endoplasmic reticulum and their pH monitoring with surface regulated carbon dots. Nanoscale 10:12788–12796
92. Zhang QQ, Yang T, Li RS, Zou HY, Li YF, Guo J, Liu XD, Huang CZ (2018) A functional preservation strategy for the production of highly photoluminescent emerald carbon dots for lysosome targeting and lysosomal pH imaging. Nanoscale 10:14705–14711
93. Liu HF, Sun YQ, Li ZH, Yang J, Aryee AA, Qu LB, Du D, Lin YH (2019) Lysosome-targeted carbon dots for ratiometric imaging of formaldehyde in living cells. Nanoscale 11:8458–8463
94. Chen S, Jia Y, Zou GY, Yu YL, Wang JH (2019) A ratiometric fluorescent nanoprobe based on naphthalimide derivative-functionalized carbon dots for imaging lysosomal formaldehyde in HeLa cells. Nanoscale 11:6377–6383
95. Zhao SJ, Wu SL, Jia QY, Huang L, Lan MH, Wang PF, Zhang WJ (2020) Lysosome-targetable carbon dots for highly efficient photothermal/photodynamic synergistic cancer therapy and photoacoustic/two-photon excited fluorescence imaging. Chem Eng J 388:124212
96. Qin HY, Sun YQ, Geng X, Zhao KR, Meng HM, Yang R, Qu LB, Li ZH (2020) A wash-free lysosome targeting carbon dots for ultrafast imaging and monitoring cell apoptosis status. Anal Chim Acta 1106:207–215
97. Singh H, Sreedharan S, Tiwari K, Green NH, Smythe C, Pramanik SK, Thomas JA, Das A (2019) Two photon excitable graphene quantum dots for structured illumination microscopy and imaging applications: lysosome specificity and tissue-dependent imaging. Chem Commun 55:521–524
98. Guo S, Sun YQ, Geng X, Yang R, Xiao LH, Qu LB, Li ZH (2020) Intrinsic lysosomal targeting fluorescent carbon dots with ultrastability for long-term lysosome imaging. J Mater Chem B 8:736–742
99. Beams HW, Kessel RG (1968) The Golgi apparatus: structure and function. Int Rev Cytol 23:209–276
100. Li RS, Gao PF, Zhang HZ, Zheng LL, Li CM, Wang J, Li YF, Liu F, Li N, Huang CZ (2017) Chiral nanoprobes for targeting and long-term imaging of the Golgi apparatus. Chem Sci 8:6829–6835
101. Wang L, Wu B, Li WT, Li Z, Zhan J, Geng BJ, Wang SL, Pan DY, Wu MH (2017) Industrial production of ultra-stable sulfonated graphene quantum dots for Golgi apparatus imaging. J Mater Chem B 5:5355–5361
102. Han JY, Burgess K (2010) Fluorescent indicators for intracellular pH. Chem Rev 110:2709–2728
103. Jia XF, Li J, Wang EK (2012) One-pot green synthesis of optically pH-sensitive carbon dots with upconversion luminescence. Nanoscale 4:5572–5575
104. Hu YP, Yang J, Tian JW, Jia L, Yu JS (2014) Waste frying oil as a precursor for one-step synthesis of sulfur-doped carbon dots with pH-sensitive photoluminescence. Carbon 77:775–782
105. Shangguan JF, He DG, He XX, Wang KM, Xu FZ, Liu JQ, Tang JL, Yang X, Huang J (2016) Label-free carbon-dots-based ratiometric fluorescence pH nanoprobes for intracellular pH sensing. Anal Chem 88:7837–7843
106. Ye XX, Xiang YH, Wang QR, Li Z, Liu ZH (2019) A red emissive two-photon fluorescence probe based on carbon dots for intracellular pH detection. Small 15:1901673
107. Stohs SJ, Bagchi D (1995) Oxidative mechanisms in the toxicity of metal ions. Free Radic Biol Med 18:321–336
108. Yang MX, Tang QL, Meng Y, Liu JJ, Feng TL, Zhao XH, Zhu SJ, Yu WX, Yang B (2018) Reversible "off-on" fluorescence of Zn^{2+}-passivated carbon dots: mechanism and potential for the detection of EDTA and Zn^{2+}. Langmuir 34:7767–7775
109. Kong DP, Yan FY, Luo YM, Ye QH, Zhou S, Chen L (2017) Amphiphilic carbon dots for sensitive detection, intracellular imaging of Al^{3+}. Anal Chim Acta 953:63–70
110. Zhang HJ, Chen YL, Liang MJ, Xu LF, Qi SD, Chen HL, Chen XG (2014) Solid-phase synthesis of highly fluorescent nitrogen-doped carbon dots for sensitive and selective probing ferric ions in living cells. Anal Chem 86:9846–9852
111. Gong XJ, Lu WJ, Paau MC, Hu Q, Wu X, Shuang SM, Dong C, Choi MMF (2015) Facile synthesis of nitrogen-doped carbon dots for Fe^{3+} sensing and cellular imaging. Anal Chim Acta 861:74–84
112. Shangguan JF, Huang J, He DG, He XX, Wang KM, Ye RZ, Yang X, Qing TP, Tang JL (2017) Highly Fe^{3+}-selective fluorescent nanoprobe based on ultra-bright N/P codoped carbon dots and its application in biological samples. Anal Chem 89:7477–7484
113. Song Y, Zhu CZ, Song JH, Li H, Du D, Lin YH (2017) Drug-derived bright and color-tunable N-doped carbon dots for cell imaging and sensitive detection of Fe^{3+} in living cells. ACS Appl Mater Interfaces 9:7399–7405
114. Atchudan R, Edison TNJI, Aseer KR, Perumal S, Karthik N, Lee YR (2018) Highly fluorescent nitrogen-doped carbon dots derived from Phyllanthus acidus utilized as a fluorescent probe for label-free selective detection of Fe^{3+} ions, live cell imaging and fluorescent ink. Biosens Bioelectron 99:303–311
115. Gao G, Jiang YW, Jia HR, Yang JJ, Wu FG (2018) On-off-on fluorescent nanosensor for Fe^{3+} detection and cancer/normal cell differentiation via silicon-doped carbon quantum dots. Carbon 134:232–243
116. Salinas-Castillo A, Ariza-Avidad M, Pritz C, Camprubí-Robles M, Fernández B, Ruedas-Rama MJ, Megia-Fernández A, Lapresta-Fernández A, Santoyo-Gonzalez F, Schrott-Fischer A, Capitan-Vallvey LF (2013) Carbon dots for copper detection with down and upconversion fluorescent properties as excitation sources. Chem Commun 49:1103–1105

117. Sotiriou GA, Pratsinis SE (2011) Engineering nanosilver as an antibacterial, biosensor and bioimaging material. Curr Opin Chem Eng 1: 3–10
118. Zuo GC, Xie AM, Li JJ, Su T, Pan XH, Dong W (2017) Large emission red-shift of carbon dots by fluorine doping and their applications for red cell imaging and sensitive intracellular Ag^{+} detection. J Phys Chem C 121:26558–26565
119. Makam P, Shilpa R, Kandjani AE, Periasamy SR, Sabri YM, Madhu C, Bhargava SK, Govindaraju T (2018) SERS and fluorescence-based ultrasensitive detection of mercury in water. Biosens Bioelectron 100:556–564
120. Yan FY, Zou Y, Wang M, Mu XL, Yang N, Chen L (2014) Highly photoluminescent carbon dots-based fluorescent chemosensors for sensitive and selective detection of mercury ions and application of imaging in living cells. Sens Actuators B Chem 192:488–495
121. Prathumsuwan T, Jamnongsong S, Sampattavanich S, Paoprasert P (2018) Preparation of carbon dots from succinic acid and glycerol as ferrous ion and hydrogen peroxide dual-mode sensors and for cell imaging. Opt Mater 86:517–529
122. Yazid SNAM, Chin SF, Pang SC, Ng SM (2013) Detection of Sn(II) ions via quenching of the fluorescence of carbon nanodots. Microchim Acta 180:137–143
123. Tabaraki R, Abdi O, Yousefipour S (2017) Green and selective fluorescent sensor for detection of Sn (IV) and Mo (VI) based on boron and nitrogen-co-doped carbon dots. J Fluoresc 27:651–657
124. Kumar A, Chowdhuri AR, Laha D, Mahto TK, Karmakar P, Sahu SK (2017) Green synthesis of carbon dots from Ocimum sanctum for effective fluorescent sensing of Pb^{2+} ions and live cell imaging. Sens Actuators B Chem 242:679–686
125. Zhang HY, Wang Y, Xiao S, Wang H, Wang JH, Feng L (2017) Rapid detection of Cr(VI) ions based on cobalt(II)-doped carbon dots. Biosens Bioelectron 87:46–52
126. Du FK, Zeng F, Ming YH, Wu SZ (2013) Carbon dots-based fluorescent probes for sensitive and selective detection of iodide. Microchim Acta 180:453–460
127. Sun S, Jiang K, Qian SH, Wang YH, Lin HW (2017) Applying carbon dots-metal ions ensembles as a multichannel fluorescent sensor array: detection and discrimination of phosphate anions. Anal Chem 89:5542–5548
128. Du FK, Min YH, Zeng F, Yu CM, Wu SZ (2014) A targeted and FRET-based ratiometric fluorescent nanoprobe for imaging mitochondrial hydrogen peroxide in living cells. Small 10:964–972
129. Li L, Rose P, Moore PK (2011) Hydrogen sulfide and cell signaling. Annu Rev Pharmacol Toxicol 51:169–187
130. Yu CM, Li XZ, Zeng F, Zheng FY, Wu SZ (2013) Carbon-dot-based ratiometric fluorescent sensor for detecting hydrogen sulfide in aqueous media and inside live cells. Chem Commun 49:403–405
131. Zhang XD, Wu FG, Liu PD, Gu N, Chen Z (2014) Enhanced fluorescence of gold nanoclusters composed of $HAuCl_4$ and histidine by glutathione: glutathione detection and selective cancer cell imaging. Small 10:5170–5177
132. Sun XH, Yang SH, Guo MZ, Ma S, Zheng MD, He J (2017) Reversible fluorescence probe based on N-doped carbon dots for the determination of mercury ion and glutathione in waters and living cells. Anal Sci 33:761–767
133. Kim DO, Lee KW, Lee HJ, Lee CY (2002) Vitamin C equivalent antioxidant capacity (VCEAC) of phenolic phytochemicals. J Agric Food Chem 50:3713–3717
134. Feng LL, Wu YX, Zhang DL, Hu XX, Zhang J, Wang P, Song ZL, Zhang XB, Tan WH (2017) Near infrared graphene quantum dots-based two-photon nanoprobe for direct bioimaging of endogenous ascorbic acid in living cells. Anal Chem 89:4077–4084
135. Kiran S, Misra RDK (2015) Mechanism of intracellular detection of glucose through nonenzymatic and boronic acid functionalized carbon dots. J Biomed Mater Res A 103:2888–2897
136. Loo AH, Sofer Z, Bousa D, Ulbrich P, Bonanni A, Pumera M (2016) Carboxylic carbon quantum dots as a fluorescent sensing platform for DNA detection. ACS Appl Mater Interfaces 8:1951–1957
137. Mahani M, Mousapour Z, Divsar F, Nomani A, Ju HX (2019) A carbon dot and molecular beacon based fluorometric sensor for the cancer marker microRNA-21. Microchim Acta 186:132
138. Han GM, Zhao J, Zhang RL, Tian XH, Liu ZJ, Wang AD, Liu RY, Liu BH, Han MY, Gao XH, Zhang ZP (2019) Membrane-penetrating carbon quantum dots for imaging nucleic acid structures in live organisms. Angew Chem Int Ed 58:7087–7091
139. Mao Y, Bao Y, Han DX, Li FH, Niu L (2012) Efficient one-pot synthesis of molecularly imprinted silica nanospheres embedded carbon dots for fluorescent dopamine optosensing. Biosens Bioelectron 38:55–60
140. Liu XQ, Wang T, Wang WJ, Zhou ZP, Yan YS (2019) A tailored molecular imprinting ratiometric fluorescent sensor based on red/blue carbon dots for ultrasensitive tetracycline detection. J Ind Eng Chem 72:100–106
141. Deng JH, Lu QJ, Hou YX, Liu ML, Li HT, Zhang YY, Yao SZ (2015) Nanosensor composed of nitrogen-doped carbon dots and gold nanoparticles for highly selective detection of cysteine with multiple signals. Anal Chem 87:2195–2203
142. Copur F, Bekar N, Zor E, Alpaydin S, Bingol H (2019) Nanopaper-based photoluminescent enantioselective sensing of L-lysine by L-cysteine modified carbon quantum dots. Sens Actuators B Chem 279:305–312

143. Han TQ, Yan T, Li YY, Cao W, Pang XH, Huang QJ, Wei Q (2015) Eco-friendly synthesis of electrochemiluminescent nitrogen-doped carbon quantum dots from diethylene triamine pentacetate and their application for protein detection. Carbon 91:144–152
144. Li Q, Ohulchanskyy TY, Liu RL, Koynov K, Wu DQ, Best A, Kumar R, Bonoiu A, Prasad PN (2010) Photoluminescent carbon dots as biocompatible nanoprobes for targeting cancer cells in vitro. J Phys Chem C 114:12062–12068
145. Zheng M, Ruan SB, Liu S, Sun TT, Qu D, Zhao HF, Xie ZG, Gao HL, Jing XB, Sun ZC (2015) Self-targeting fluorescent carbon dots for diagnosis of brain cancer cells. ACS Nano 9:11455–11461
146. Bhunia SK, Maity AR, Nandi S, Stepensky D, Jelinek R (2016) Imaging cancer cells expressing the folate receptor with carbon dots produced from folic acid. ChemBioChem 17:614–619
147. Zhang XD, Chen XK, Yang JJ, Jia HR, Li YH, Chen Z, Wu FG (2016) Quaternized silicon nanoparticles with polarity-sensitive fluorescence for selectively imaging and killing Gram-positive bacteria. Adv Funct Mater 26:5958–5970
148. Lin FM, Bao YW, Wu FG (2019) Carbon dots for sensing and killing microorganisms. C 5:33
149. Mehta VN, Jha S, Kailasa SK (2014) One-pot green synthesis of carbon dots by using Saccharum officinarum juice for fluorescent imaging of bacteria (Escherichia coli) and yeast (Saccharomyces cerevisiae) cells. Mater Sci Eng C 38:20–27
150. Nandi S, Ritenberg M, Jelinek R (2015) Bacterial detection with amphiphilic carbon dots. Analyst 140:4232–4237
151. Yang JJ, Zhang XD, Ma YH, Gao G, Chen XK, Jia HR, Li YH, Chen Z, Wu FG (2016) Carbon dot-based platform for simultaneous bacterial distinguishment and antibacterial applications. ACS Appl Mater Interfaces 8:32170–32181
152. Yang JJ, Gao G, Zhang XD, Ma YH, Chen XK, Wu FG (2019) One-step synthesized carbon dots with bacterial contact-enhanced fluorescence emission property: fast Gram-type identification and selective Gram-positive bacterial inactivation. Carbon 146:827–839
153. Chandra S, Mahto TK, Chowdhuri AR, Das B, Sahu SK (2017) One step synthesis of functionalized carbon dots for the ultrasensitive detection of Escherichia coli and iron (III). Sens Actuators B Chem 245:835–844
154. Chandra S, Chowdhuri AR, Mahto TK, Samui A, Sahu SK (2016) One-step synthesis of amikacin modified fluorescent carbon dots for the detection of Gram-negative bacteria like *Escherichia coli*. RSC Adv 6:72471–72478
155. Chen XK, Zhang XD, Li CC, Sayed SM, Sun W, Lin FM, Wu FG (2019) Superbright organosilica nanodots as a universal sensor for fast discrimination and accurate quantification of live/dead cells. Sens Actuators B Chem 295:49–55
156. Lu F, Song YX, Huang H, Liu Y, Fu YJ, Huang J, Li H, Qu HH, Kang ZH (2017) Fluorescent carbon dots with tunable negative charges for bio-imaging in bacterial viability assessment. Carbon 120:95–102
157. Chen XK, Zhang XD, Lin FM, Guo YX, Wu FG (2019) One-step synthesis of epoxy group-terminated organosilica nanodots: a versatile nanoplatform for imaging and eliminating multidrug-resistant bacteria and their biofilms. Small 15:1901647
158. Ritenberg M, Nandi S, Kolusheva S, Dandela R, Meijler MM, Jelinek R (2016) Imaging Pseudomonas aeruginosa biofilm extracellular polymer scaffolds with amphiphilic carbon dots. ACS Chem Biol 11:1265–1270
159. Ran HH, Cheng XT, Bao YW, Hua XW, Gao G, Zhang XD, Jiang YW, Zhu YX, Wu FG (2019) Multifunctional quaternized carbon dots with enhanced biofilm penetration and eradication efficiencies. J Mater Chem B 7:5104–5114
160. Belkahla H, Boudjemaa R, Caorsi V, Pineau D, Curcio A, Lomas JS, Decorse P, Chevillot-Biraud A, Azaïs T, Wilhelm C, Randriamahazaka H, Hémadi M (2019) Carbon dots, a powerful non-toxic support for bioimaging by fluorescence nanoscopy and eradication of bacteria by photothermia. Nanoscale Adv 1:2571–2579
161. Zhang ML, Hu LL, Wang HB, Song YX, Liu Y, Li H, Shao MW, Huang H, Kang ZH (2018) One-step hydrothermal synthesis of chiral carbon dots and their effects on mung bean plant growth. Nanoscale 10:12734–12742
162. Wang ZY, Qu YN, Gao XT, Mu CJ, Bai JP, Pu QS (2014) Facile preparation of oligo(ethylene glycol)-capped fluorescent carbon dots from glutamic acid for plant cell imaging. Mater Lett 129:122–125
163. Li W, Zhang HR, Zheng YJ, Chen S, Liu YL, Zhuang JL, Liu WR, Lei BF (2017) Multifunctional carbon dots for highly luminescent orange-emissive cellulose based composite phosphor construction and plant tissue imaging. Nanoscale 9:12976–12983
164. Tripathi S, Sarkar S (2014) Influence of water soluble carbon dots on the growth of wheat plant. Appl Nanosci 5:609–616
165. Pan LL, Sun S, Zhang L, Jiang K, Lin HW (2016) Near-infrared emissive carbon dots for two-photon fluorescence bioimaging. Nanoscale 8:17350–17356
166. Lan MH, Zhao SJ, Zhang ZY, Yan L, Guo L, Niu GL, Zhang JF, Zhao JF, Zhang HY, Wang PF, Zhu GY, Lee CS, Zhang WJ (2017) Two-photon-excited near-infrared emissive carbon dots as multifunctional agents for fluorescence imaging and photothermal therapy. Nano Res 10:3113–3123
167. Lu SY, Sui LZ, Liu JJ, Zhu SJ, Chen AM, Jin MX, Yang B (2017) Near-infrared photoluminescent polymer–carbon nanodots with two-photon fluorescence. Adv Mater 29:1603443
168. Yang CH, Zhu SJ, Li ZL, Li Z, Chen C, Sun L, Tang W, Liu R, Sun Y, Yu M (2016) Nitrogen-doped carbon dots with excitation-independent

long-wavelength emission produced by a room-temperature reaction. Chem Commun 52:11912–11914
169. Wu ZL, Liu ZX, Yuan YH (2017) Carbon dots: materials, synthesis, properties and approaches to long-wavelength and multicolor emission. J Mater Chem B 5:3794–3809
170. Shamsipur M, Barati A, Karami S (2017) Long-wavelength, multicolor, and white-light emitting carbon-based dots: achievements made, challenges remaining, and applications. Carbon 124:429–472
171. Li QJ, Zhou M, Yang QF, Wu Q, Shi J, Gong AH, Yang MY (2016) Efficient room-temperature phosphorescence from nitrogen-doped carbon dots in composite matrices. Chem Mater 28:8221–8227
172. Jiang K, Wang YH, Cai CZ, Lin HW (2018) Conversion of carbon dots from fluorescence to ultralong room-temperature phosphorescence by heating for security applications. Adv Mater 30:1800783
173. Jiang K, Gao XL, Feng XY, Wang YH, Li ZJ, Lin HW (2020) Carbon dots with dual-emissive, robust, and aggregation-induced room-temperature phosphorescence characteristics. Angew Chem Int Ed 59:1263–1269
174. Jiang L, Ding HZ, Lu SY, Geng T, Xiao GJ, Zou B, Bi H (2020) Photoactivated fluorescence enhancement in F,N-doped carbon dots with piezochromic behavior. Angew Chem Int Ed 59:9986–9991
175. Lu SY, Xiao GY, Sui LZ, Feng TL, Yong X, Zhu SJ, Li BJ, Liu ZY, Zou B, Jin MX, Tse JS, Yan H, Yang B (2017) Piezochromic carbon dots with two-photon fluorescence. Angew Chem Int Ed 56:6187–6191
176. Zhan Y, Geng T, Liu YL, Hu CF, Zhang XJ, Lei BF, Zhuang JL, Wu X, Huang D, Xiao GJ, Zou B (2018) Near-ultraviolet to near-infrared fluorescent nitrogen-doped carbon dots with two-photon and piezochromic luminescence. ACS Appl Mater Interfaces 10:27920–27927
177. Zhu SJ, Zhang JH, Tang SJ, Qiao CY, Wang L, Wang HY, Liu X, Li B, Li YF, Yu WL, Wang XF, Sun HC, Yang B (2012) Surface chemistry routes to modulate the photoluminescence of graphene quantum dots: from fluorescence mechanism to up-conversion bioimaging applications. Adv Funct Mater 22:4732–4740
178. Alam AM, Park BY, Ghouri ZK, Park M, Kim HY (2015) Synthesis of carbon quantum dots from cabbage with down-and up-conversion photoluminescence properties: excellent imaging agent for biomedical applications. Green Chem 17:3791–3797
179. Li JY, Liu Y, Shu QW, Liang JM, Zhang F, Chen XP, Deng XY, Swihart MT, Tan KJ (2017) One-pot hydrothermal synthesis of carbon dots with efficient up- and down-converted photoluminescence for the sensitive detection of morin in a dual-readout assay. Langmuir 33:1043–1050